Chapter 9

# MOLECULAR CHEMISORPTION

H.-J. FREUND and M. NEUMANN

## 1. INTRODUCTION

The study of adsorption of molecules on surfaces with photoelectron spectroscopy starts in the vicinity of 1971 with the landmark paper by Eastman and Cashion (ref. 1) on the system CO/Ni. Still much of present research on molecular adsorption is being done on CO adsorbates or co-adsorbates with electronegative and electropositive additives. The adsorption behaviour of other diatomics, e.g. $N_2$ and NO, has also been investigated thoroughly by ARUPS as reviewed in (refs.2,3). During the last 15 years, larger molecules have been studied by means of ARUPS, for example unsaturated hydrocarbons like acetylene, ethylene, benzene just to name a few (ref. 4). Reactive systems have been investigated using ARUPS with varying success. None of these adsorbate systems has been analysed in any such detail as CO adsorbates. This means that much of the fundamental aspects of ARUPS of molecular chemisorption systems can be demonstrated using experimental results on CO adsorbate systems. Therefore, we use CO adsorbates to illustrate some basic principles. On these grounds we then discuss specific aspects of ARUPS on molecular adsorbates and co-adsorbates by using examples of more complicated systems. In an attempt to order the various aspects of ARUPS on molecular chemisorption systems we have devided the present review into two parts, i.e. one covering the molecular aspects including co-adsorption, and a second one dealing with intermolecular interaction in connection with the formation of two-dimensionally ordered overlayers. A subdivision in this manner is natural because molecular chemisorption is determined essentially by these two types of interactions.

Fig.1 illustrates on the basis of one-electron level diagrams how the molecule substrate and the intermolecular interactions

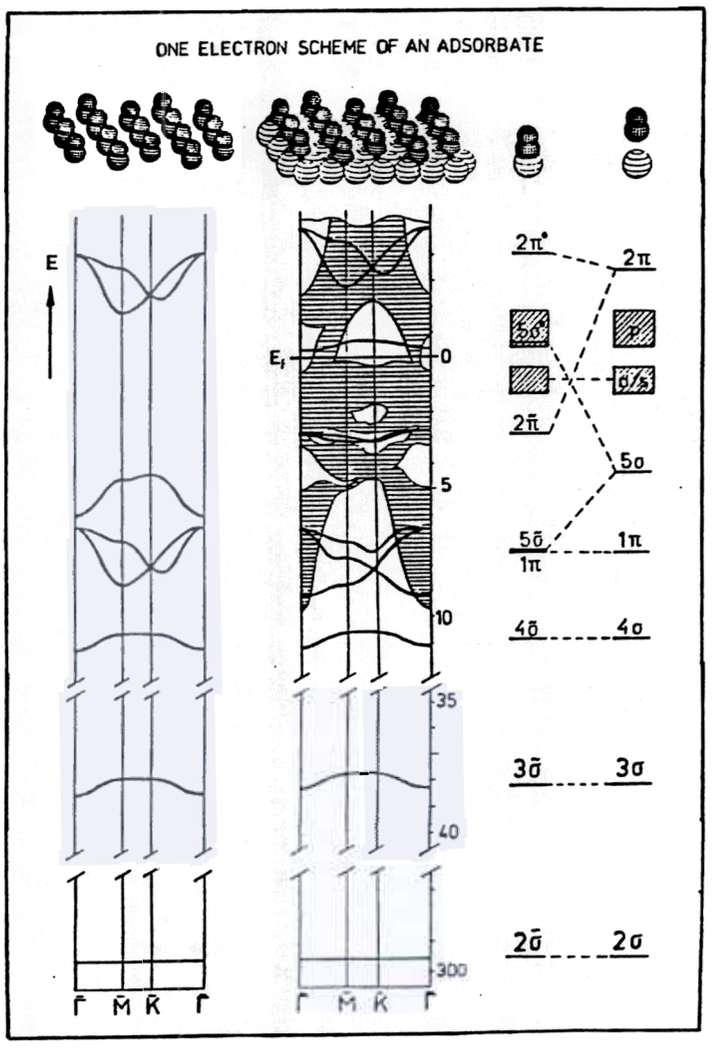


Fig. 1. Schematic one-electron level diagrams for diatomic molecules (CO) interacting with a transition metal surface. The level scheme for a molecule-metal cluster (right) is correlated with the band scheme of a free unsupported molecular layer (extreme left) and the band scheme of the quasi-twodimensional adsorbate (middle). The band structure of the metal projected onto the surface is schematically shown as the hatched area.

affect the electronic states of the adsorbate. It shows on the right hand side a one-electron level diagram for a single isolated CO molecule correlated with a level diagram of a CO molecule interacting with a single metal atom or a small metal cluster. The electronic states of the system can be classified according to the point group of the CO-metal cluster. On the left hand side the band structure of an isolated CO overlayer is shown and compared in the middle with the full band structure of the CO adsorbate on a fcc(111) single crystal metal surface. In this case the point group of the local CO-metal site is not sufficient to characterize the electronic states of the system. The full global space group of the periodic arrangement has to

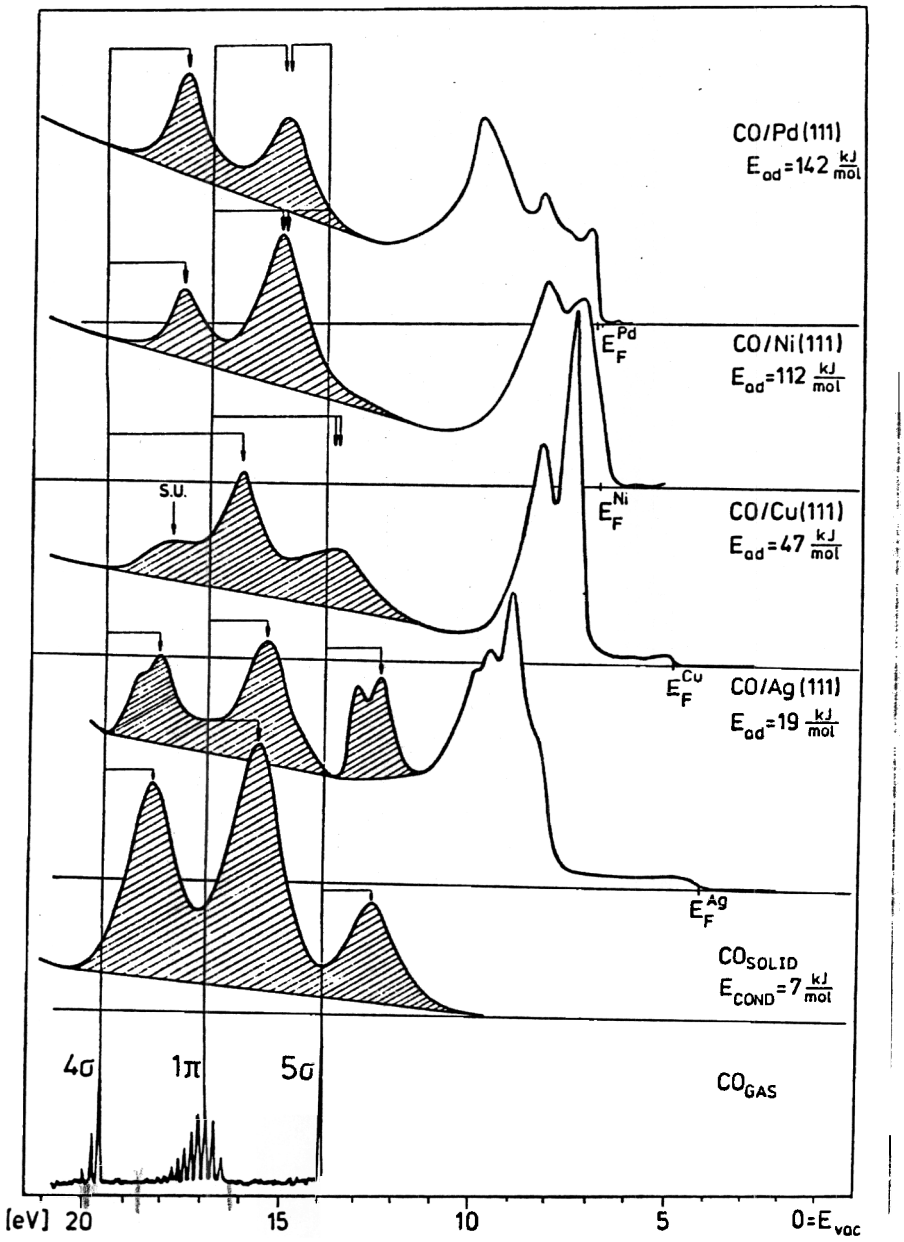


Fig. 2. Set of normal emission CO adsorbate spectra (refs. 8-13). s.u.: shake up satellite.

be considered. Clearly, the relative magnitudes of molecule-substrate and intermolecular interaction potential determine whether local or global symmetry dominates. Since ARUPS, as will be shown further below, allows us to study symmetry properties of the electronic states of adsorbate systems, it may be possible to disentangle via ARUPS in favourable cases which of these two types of interactions and how they are active in the adsorbate. We note at this point that all of our examples refer to adsorbate systems on transition metal single crystal surfaces, because the majority of data is available for these systems. There are very few examples for ARUPS studies of molecular adsorbates on semiconductor surfaces (ref. 5).

## 2. MOLECULAR ASPECTS

Let us start with the "molecular aspect" of the CO-molecule-substrate interaction, i.e. the right hand side of Fig.1. What happens electronically can easily be explained in terms of the so called Blyholder model (ref. 6): The carbon lone pair is donated into empty d or s levels of the metal atom, establishing a $\sigma$ metal-molecule interaction. Synenergetically, metal $\pi$-electrons are donated into empty molecular orbitals ($2\pi^*$) of CO forming a $\pi$ metal-molecule interaction. From the view point of the molecule we can look at this process as a $\sigma$-donation-$\pi$-back-donation process. This means that the distribution of electrons among the subsystems, i.e. CO molecule and metal atom, in the metal-CO-cluster is considerably different as compared with the non-interacting subsystems. For example, the electron configuration of the metal atom in the cluster may be different from the isolated metal atom, or the electron distribution within the CO molecule bonded towards the metal atom may look more like the electron distribution of an "excited" CO molecule rather than the ground state CO molecule (ref. 7). Nevertheless, as a consequence of the relatively weak molecule-substrate interaction only certain electronic levels of the subsystems are strongly influenced, so that it appears to be justified to classify the electronic levels of the interacting adsorbate system according to the nomenclature used for the isolated subsystems. Naturally, the distortions of the molecular as well as the metal levels are reflected by changes in the ionization energies of those levels, their ionization probabilities, and the line shapes of the ionization bands. Fig.2 shows a set of angle resolved, normal emission valence electron spectra of CO adsorbates on different single crystal surfaces (refs. 8-13). The binding energy ($E_B = h\nu - E_{kin}$) refers to the vacuum level. (Often the binding energy is referenced to the Fermi-level ($E_F$) of the system. The binding energies with respect to the Fermi and to the vacuum levels are connected via the workfunction $\Phi$ of the adsorbate system.) The region where we expect emission from the three outer valence levels of CO, i.e. the $5\sigma$, $1\pi$, and $4\sigma$ levels (see Fig.1) is shown, and most of the following discussion will concentrate on these levels. From the bottom to the top the heat of adsorption increases from 19kJ/mol to 142 kJ/mol (refs. 14-18). This is accompanied by changes in the adsorbate spectra as compared to the gas and solid phase

spectra which are shown for comparison. There are several interesting differences in binding energies, line intensities and line shapes between gas, condensed and adsorbate phases, which we shall comment on in the following. In order to do so we have to cover many different aspects such as symmetry considerations, relaxation energies, line widths, shake-up satellites, and so on. We shall use Fig.2 as a guide line to discuss the various aspects as they occur in going from the gas phase via weakly chemisorbed to strongly chemisorbed adsorbates.

In CO/Ag(111) at T=20K CO is physisorbed as documented by the small $E_{ad}$=19 kJ/mole (ref. 15). This explains why a spectrum similar to condensed CO is observed for this adsorbate. The splittings in the 4σ and 5σ emissions are connected with the formation of a two dimensional overlayer as will be discussed in the second part of this review. In comparison with the gas phase, however, rather dramatic changes are observed upon condensation and physisorption, namely a shift of about 1 eV towards lower binding energies and a considerable increase in line width which destroys the vibrational structure observed in the gas phase. Chiang et al. (ref. 19) found shifts by comparing the photoelectron spectra of CO, adsorbed on a metal surface (Al(111)), and of CO adsorbed on the same surface precovered with a monolayer of Xe, so to say as a spacer between metal and CO. Fig.3 shows the spectra as a function of increasing thickness of the Xe spacer. Clearly, the bands shift towards higher binding energies, and appear to exhibit smaller line widths when well separated from the surface. Theories have been developed that allow one to understand these observations on the basis of hole hopping and relaxation together with adsorbate-surface vibrations within the condensed quasi-two- or three-dimensional molecular solids (refs. 20-22). The shift of the band to lower binding energy is a consequence of the electronic relaxation in the final ion state, which is considerably more pronounced when the molecule is bound to a readily polarizable medium, because metal electrons screen the positive charge introduced by the ionization process more effectively than do the electrons on the isolated molecule. The more pronounced screening stabilizes the final hole state relative to the initial state, which lowers the binding energy as observed. Measured temperature dependences of line widths in molecular solids and model systems support the developed theoretical ideas

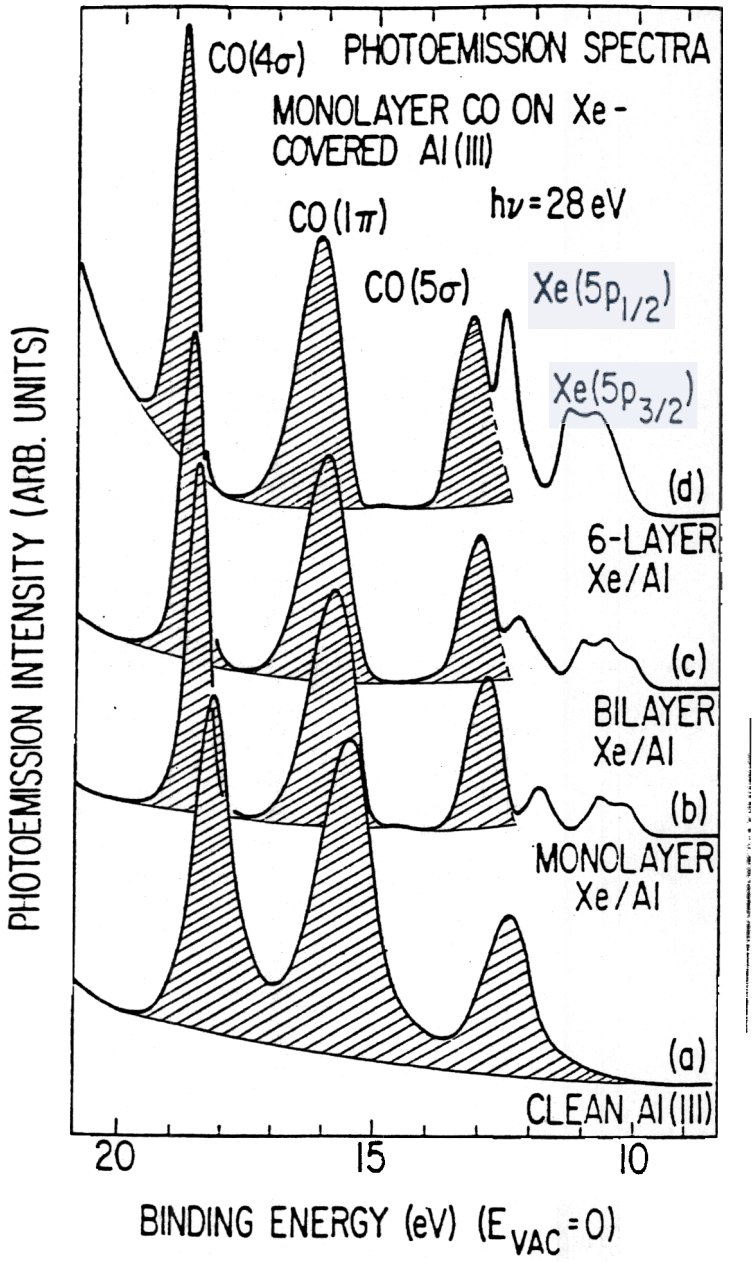


Fig. 3. Spectra of CO interacting with a clean and Xe precovered Al(111) surface (ref.19). The number of precovered Xe layers is indicated.

(refs. 22-23). It is likely that other processes, for example Auger decay or other radiationless decay mechanisms, contribute to these line widths as well.

If the heat of adsorption increases to about 47 kJ/mole (ref. 16) (weakly chemisorbed), like, for example, in the case of a CO adsorbate on a Cu(111) surface, the features in the spectrum shift and the intensities of the lines are altered considerably with respect to the physisorbate. The line widths, on the other hand, are quite comparable in both systems. Three lines are still found, but their assignment is, as we shall see further below, quite different from the one for the condensed molecular

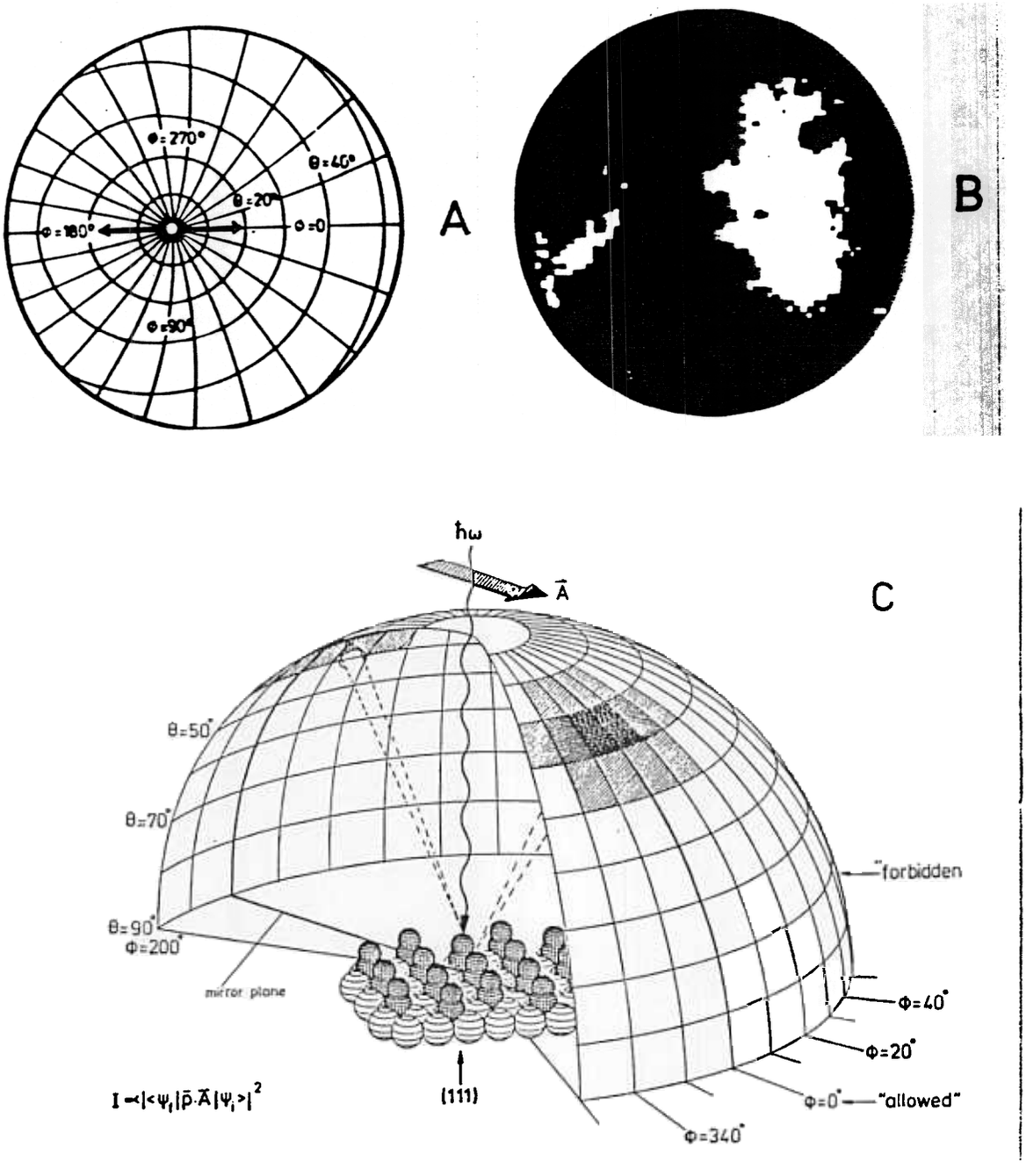


Fig. 4. CO 4σ emission intensity from CO/Pd(111) as recorded with an elliptical mirror analyser (ref. 30). a) polar diagram, the direction of the light polarization vector is indicated by an arrow. b) intensity distribution pattern. Light regions correspond to high emission current. c) Quasi three dimensional representation of the relation between geometric structure of the adsorbate and the measured 4σ emission intensity as a function of ϕ and Θ. The emission intensity is given by the shaded areas.

solid.

Before we discuss how ARUPS establishes this assignment let us first turn towards the spectra of the strongly chemisorbed adsorbate systems, i.e. CO/Ni(111) and CO/Pd(111)- which are

only two examples out of a wealth of experimental data (refs. 24-40). In the case of strong chemisorption the spectra show two bands, the binding energies of which are rather independent of the particular system under consideration, but are shifted by more than 2 eV to lower values with respect to the gas phase. ARUPS has been instrumental to show that these two CO induced bands are really caused by three CO ion states, and that the CO molecules are oriented with their axis parallel to the surface normal (ref. 24). Fig. 4b shows an angular distribution pattern for the 4σ ion state intensity of a CO/Pd(111) adsorbate as recorded with an elliptical mirror analyser employing polarized synchrotron light (ref. 30). The polarization plane is placed along the 0°/180°-azimuth, i.e. the horizontal line in the angular coordinate diagram shown in Fig. 4a. With respect to the Pd(111) surface this corresponds to a mirror plane of the system. Figure 4c shows a quasi-three-dimensional plot of the emission intensity distribution (shaded areas on the half-sphere) as a function of azimuthal (Φ) and polar (Θ) angles in direct relation to the geometric structure of the molecular adsorbate. The angular distribution pattern clearly shows how the symmetry of the adsorbate wavefunction with respect to this mirror plane determines the angular distribution of the emitted electron current. The reason for this remarkable behaviour has been discussed long before by several groups (refs. 24,25,41) on the basis of symmetry considerations for the photoemission matrix element (refs. 42-43):

$$I \alpha | \langle \Psi_f | p | \Psi_i \rangle |^2 \qquad (1)$$

and we shall briefly repeat the arguments:

Firstly it has to be remembered that $\Psi_f$ is the final state after electron excitation consisting of the ion state $^{N-1}\Psi_{e,E}$ and the emitted electron $\Phi_e(n)$, and $\Psi_i$ represents the neutral ground state of the system. Since p is a one electron operator the matrix element can be rewritten as (ref. 44):

$$I \alpha \sum_{k,E} \langle \Phi_e(n) | p_n | \Phi_k(n) \rangle \langle ^{N-1}\Psi_{e,E} | a_k \Psi_i \rangle |^2 \qquad (2)$$

where $a_k$ and $\Phi_k(n)$ are the annihilation operator and the one-electron wave function of the electron that is being emitted, respectively. These $\Phi_k(n)$ are called initial states in the following. The first matrix element determines the angular distribution pattern, the second matrix element defines the absolute value and contains the internal degrees of freedom of

the system, e.g. the line widths. The sum takes all possible ion states $^{N-1}\Psi_{e,E}$ into account and explains the existence of satellite structure (ref. 44). Since we are interested in ARUPS, much of the discussion will concentrate on the first matrix element. Secondly, in order to evaluate whether this matrix element is finite, and thus leads us to expect a finite photoelectron current into a specific direction in space, symmetry arguments can be used. In principle the space group of the adsorbate under consideration has to be chosen, and then we have to classify the wavefunctions according to its irreducible representations. Often, it is sufficient to consider one specific symmetry operation belonging to the point group, instead of all possible symmetry operations, in order to predict the angular variations of electron emission. In the present case we refer to one of the mirror planes of the Pd(111) surface. If we classify the wavefunctions of the electron $\Phi_e$ and $\Phi_k$, as well as the momentum operator p "even" or "odd" with respect to this mirror plane, we are in the position to differentiate between "even" and "odd" initial states by choosing certain light polarizations and detecting the angular distribution pattern as long as spin orbit interaction is not important (ref. 45). For the above given situation the light polarization direction is within the mirror plane. This corresponds to even symmetry of the momentum operator. Therefore, initial states with even symmetry will emit into the direction of the mirror plane because the final states have to be even in order for the matrix element not to vanish. In principle, one would expect a finite emission probability along the whole mirror plane. In the present case, however, one has to take into account the cylindrical symmetry of a CO molecule, bonded linearly towards the metal surface. Even initial states of a cylindrical molecule cannot emit into a direction given by the plane perpendicular to the mirror plane which contains the light polarization vector. This latter property can easily be understood if we remember that any plane in a cylindrical system containing the cylindrical axis is a symmetry plane. Combining this property with the fact that the momentum operator is odd with respect to this second plane means that there cannot be any emission of even states into this direction. Therefore, in order to fulfill both conditions simultaneously, we do not expect an intense CO-4$\sigma$ emission along the surface normal for

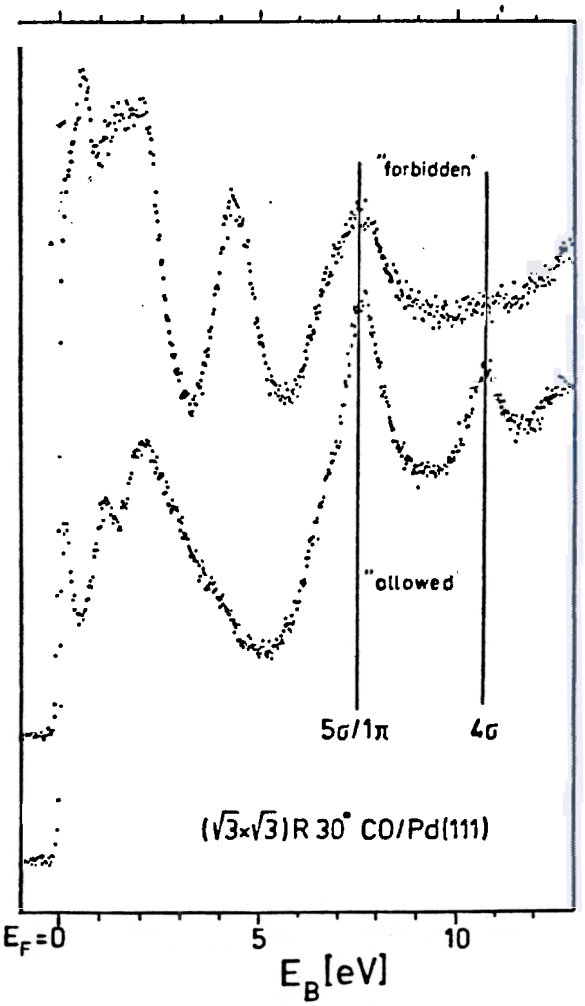


Fig. 5. ARUP-spectra of CO/Pd(111) in "forbidden" and "allowed" geometry (see text). The CO induced features are marked. Pd emissions show strong symmetry related intensity variations as well (ref. 13). The light polarization was placed along a Pd(210) mirror plane.

light polarized in the surface plane. 4σ emission along the surface normal can only be achieved by using a light polarization perpendicular to the surface plane because in this case the momentum operator is even with respect to any plane perpendicular to the surface plane. If we combine the considerations so far we verify the above angular distribution pattern.

As a consequence of the outlined behaviour of even initial states, we expect a complementary behaviour of odd initial states. This is exactly what is observed experimentally and is shown as a set of electron distribution curves- which is the usual way to look at ARUP-spectra-in Fig.5. In this figure the complementary behaviour of σ- and π-emissions, which was first observed by Plummer and coworkers (ref. 24) is obvious: If we

record a spectrum perpendicular (so called "forbidden" geometry) to the incidence plane we do not observe emission in the region of the 4σ level but only in the region of the 5σ/1π levels. Note, that the 1π-ion state of CO has two degenerate components, one of which always transforms according to the even representation. Thus, we expect to see the one odd component of the 1π-ion state. A spectrum recorded with the analyser placed within the incidence plane, the so called "allowed" geometry, show all states with even symmetry. From Fig.5 it is clear that the band at 8 eV below the Fermi energy (Fig.2) contains two states, i.e. the 1π and the 5σ ion states. Their energies are, in contrast to the gas phase, nearly (within a few tenths of an eV) degenerate in the adsorbate. This is a situation, predicted by the simple one-electron level scheme in Fig.1. It is due to the donation of the 5σ carbon lone pair into empty metal levels, thus stabilizing the CO 5σ level with respect to the 1π level which is not as intimately involved in the molecule metal interaction for linear metal-molecule bonding.

The logic so far has been that we have assumed a geometry of the adsorbate site, thus knowing the symmetry of the system, i.e. CO perpendicular to the surface plane, and have verified this via an analysis of the angular photoemission spectra. Usually, the arguments are turned around, namely, the observed angular behaviour is used to deduce an adsorbate site symmetry.

The adsorbate induced features exhibit, in addition to the described angular dependences (ref. 46), characteristic photon energy dependences, which, when recorded in an angle dependent fashion, can be used to get further information about adsorbate site geometry (ref. 24). Fig.6 shows a plot of the intensity of the 4σ ion state as a function of photon energy. The data have been recorded for the system CO/Co(0001) (ref. 27) for three different electron emission angles. The observed resonance feature is caused by the so called shape resonance, which is well known from CO gas phase studies (ref. 47). It can be traced back to a molecular final state of σ symmetry in the ionization continuum, quasi-bound by a centrifugal barrier in the molecular potential. Its symmetry confines the electron emission direction to the molecular axis, and directs the 4σ emission out of the oxygen end of the molecule. This means that for the case of a molecule oriented along the surface normal, carbon-end bound to the surface, the resonance should peak along the surface normal.

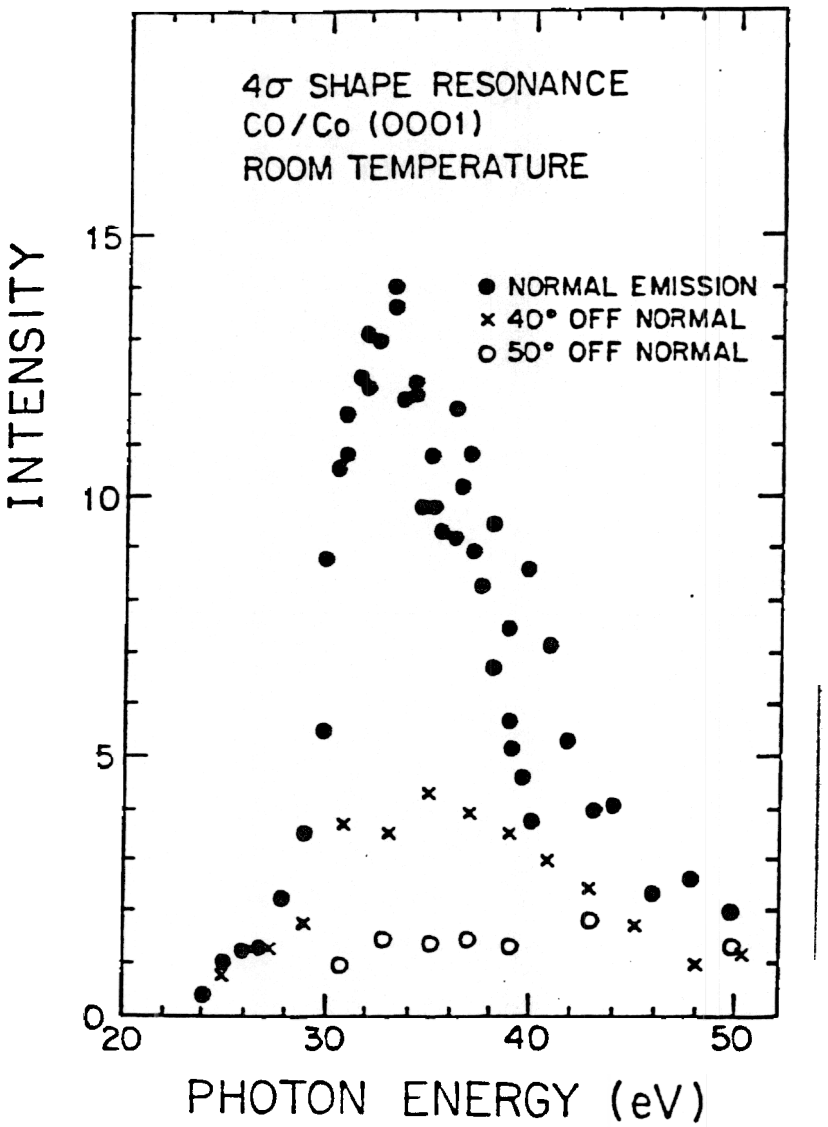


Fig. 6. Intensity variations of the 4σ intensity in CO/Co(0001) as a function of photon energy. Filled circles refer to normal emission, open circles and crosses to off-normal emission as indicated (ref. 27).

Experimentally, we find in Fig.6 the expected behaviour, i.e. a pronounced attenuation of the resonance intensity for off normal emission, which corroborates the assumed adsorbate orientation. Another interesting property of this resonance is its coherent-forward-emission character (ref. 48). Coherent-forward-emission leads to an oscillatory behaviour of the photoionization cross-section. The periodicity is determined by the distance of the interfering sources, which are in the present case the carbon and oxygen atoms participating in the ion state wavefunction under consideration (4σ). Examples are shown in Fig.7 for the system CO/Pd(111) and CO+Na/Pd(111) (ref. 49). At a photon energy of 35 eV the resonance corresponding to the one shown in

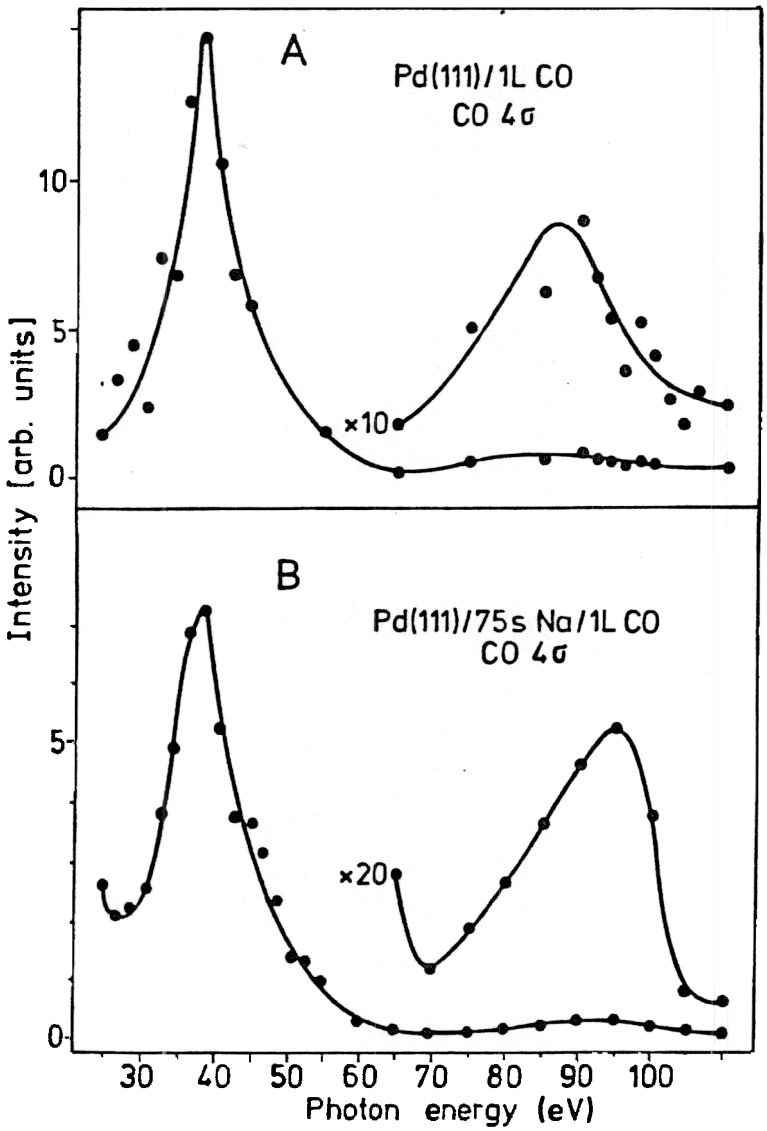


Fig. 7. Intensity variations in normal emission of the CO 4σ intensity in (a) CO/Pd(111) and (b) CO+Na/Pd(111) as a function of photon energy between 25 eV and 110 eV (ref. 49).

Fig.6 is found. As predicted by theoretical calculations (ref. 48), at about 95 eV a second feature with larger width and smaller amplitude is observed. Potentially, the energy separation can be used to estimate the CO bond length in adsorbates as proposed by Gustafsson (ref. 48). Very similar results as those discussed so far for the 4σ ion state are found for the 5σ ion state. A comparison of the resonance positions in different CO systems shows (refs. 49-51) that it is not so much dependent on the specific system, as was originally expected, and its absence is somewhat surprising on the basis of current theoretical models.

If we apply the geometry sensitive experiments, just presented, to investigate the geometric structure of physisorbed

molecules, for example CO/Ag(111) (ref. 10), Fig.2 or CO/Al(111) (ref. 19), Fig.3, we find that the orientation of the molecular axis is not, like in the chemisorbates perpendicular, but rather parallel to the surface. The reason is that due to the electronic structure of the substrate, not enough energy can be gained via the above mentioned σ-donor-π-acceptor interaction, for which a vertical orientation is a neccessary prerequisite. As we shall see further below, intermolecular interactions are rather important to understand the electronic structure of physisorbates.

At this point we can return to the assignment and analysis of the spectra of the weakly chemisorbed system. The assignment of the spectrum of the CO/Cu(111) system, given in Fig.2 indicates that the considerations presented so far are not complete and sufficient to explain all experimental findings. It has been shown theoretically that for weakly chemisorbed systems so called shake up excitations accompanying the "normal" electron emission have to be considered (refs. 52-56). These shake up excitations are manifestations of the fact that the ionization process is a rather complicated many-electron process (refs. 44, 57). They can be assigned to electron excitations in addition to electron emission. Their intensity is determined by the second matrix element in equation (2) whose magnitude is governed by the projection of the wavefunction of the shake-up state $^{N-1}\Psi_{e,E}$ onto the "frozen" ion state $a_k\Psi_i$. Shake-up intensities are rather low for chemisorbed and for physisorbed systems but reach the maximum for intermediate metal-molecule coupling, i.e. weak chemisorption (refs. 53-58). Again, ARUPS can be employed to support the assignment as given in Fig.2 for the CO/Cu(111) system. If the most intense CO features were due to 1π emission, as might be suspected by comparing the spectra of the CO/Cu(111) system with CO/Ag(111), a resonance behaviour for this particular peak would not be allowed. Horn et al. (ref. 59) showed that both bands at higher binding energy are due to states of σ symmetry by investigating the shape resonance discussed above. The 4σ ion state as well as the accompanying shake up transition exhibited parallel resonance behaviour as expected according to the assignment in Fig.2. A spectrum rather similar to the one of the CO/Cu system, but with even slightly more intense satellite structure, has been found for the system CO/Au (ref. 60). In the latter system the adsorption energy is

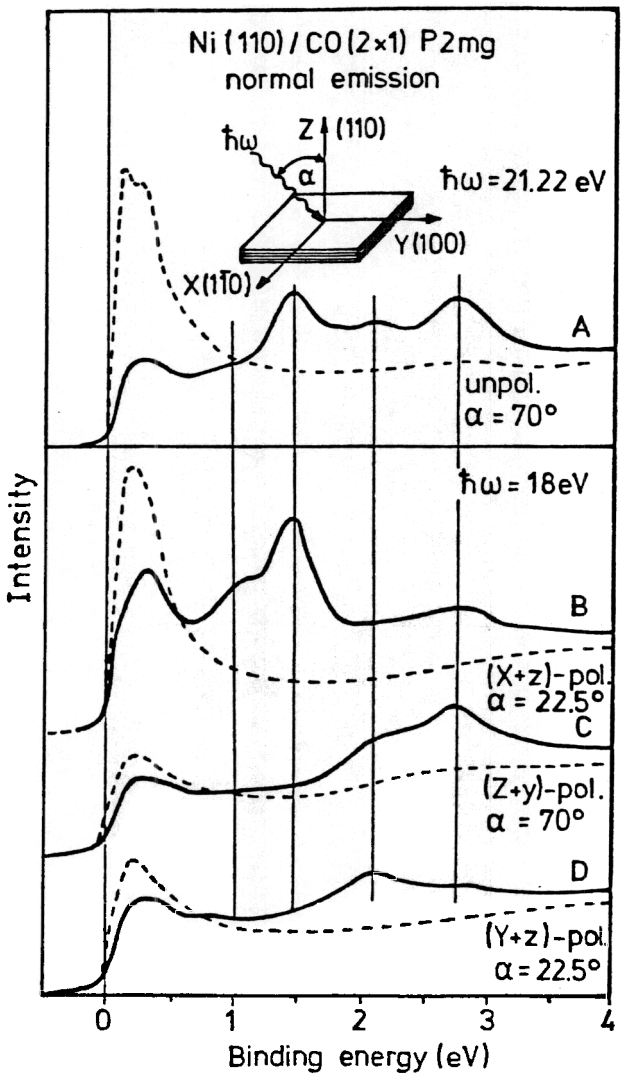


Fig. 8. ARUP-spectra in normal emission for different light polarization directions of CO(2x1)p2mg/Ni(110) (full lines) in comparison with the clean Ni(110) surface (broken lines) in the region of the metal emissions (ref. 63).

between the one for CO/Ag and CO/Cu which leads us to expect more intense satellites, and corroborates the ideas presented.

In our discussion so far we have only considered the molecule induced peaks at binding energies higher than the metal states, i.e. those states that correspond to "molecular" ion states. However, as is obvious from Fig.1 there are levels of the adsorbate system within the region of the metal projected density of states, due to the coupling of unoccupied molecular states to occupied metal states. There have been several attempts to identify these states (refs. 61-63). The most recent one was done on the system CO(2x1)p2mg/Ni(110), whose structure will be discussed in detail in connection with intermolecular interactions (ref. 26). The symmetry and high CO density of this system allows to measure the adsorbate induced

peaks in the d-band region of the Ni substrate (ref. 63). Fig.8 shows a selected set of spectra that demonstrate the intensity, symmetry and energy position of the CO induced, d-like states for this system. The spectra of the clean surface are given as dashed curves for comparison. The usually dominant CO molecular ionizations (ref. 26) are not shown in this figure. The various peak intensities are strongly polarization dependent, and, together with the measured dispersion, discussed in the section intermolecular interactions, support an assignment of these features to CO-2π-Ni-3d states.

To summerize the results so far, the ARUP-spectra are found to reflect the bonding with the surface. It is possible to differentiate between physisorbed, weakly chemisorbed, and strongly chemisorbed CO adsorbates. However, the differences in the habit of the spectra for various chemisorbed systems are rather unpronounced which limits the applicability of photoemission with respect to fingerprinting. On the other hand, ARUPS is sensitive to the local site symmetry via the angular emission pattern, as well as the angular dependence of resonance features in the ionization cross-section. For special cases the back-bonding states in the region of the metal substrate states can be identified.

In order to appreciate in more detail how these aspects of photoemission have been used to study molecule surface interactions under the influence of variations of the substrate and co-adsorbed species we briefly review selected results of adsorbates on clean and precovered surfaces:

## 2.1 Pure adsorbates

### 2.1.1 $H_2$

Even though $H_2$ adsorbates have a lot of appeal to be the model system to study molecular adsorption very little has been done with respect to the application of ARUPS. The reason is, of course, that in general, at routinely accessible temperatures hydrogen adsorbs dissociatively to form atomic adsorbates. To our knowledge only angle integrated spectra have been published for adsorbed molecular $H_2$ (ref. 64). Whether one should look at hydrogen adsorbates with coverage $\Theta=2$ as containing atomic (2H) or quasimolecular $H_2$ is probably a matter of semantics. Christmann et al. (ref. 65) have studied these systems with ARUPS and observed band dispersions as large as 4 eV and binding

energies for the hydrogen induced features close to 10 eV below $E_F$ .

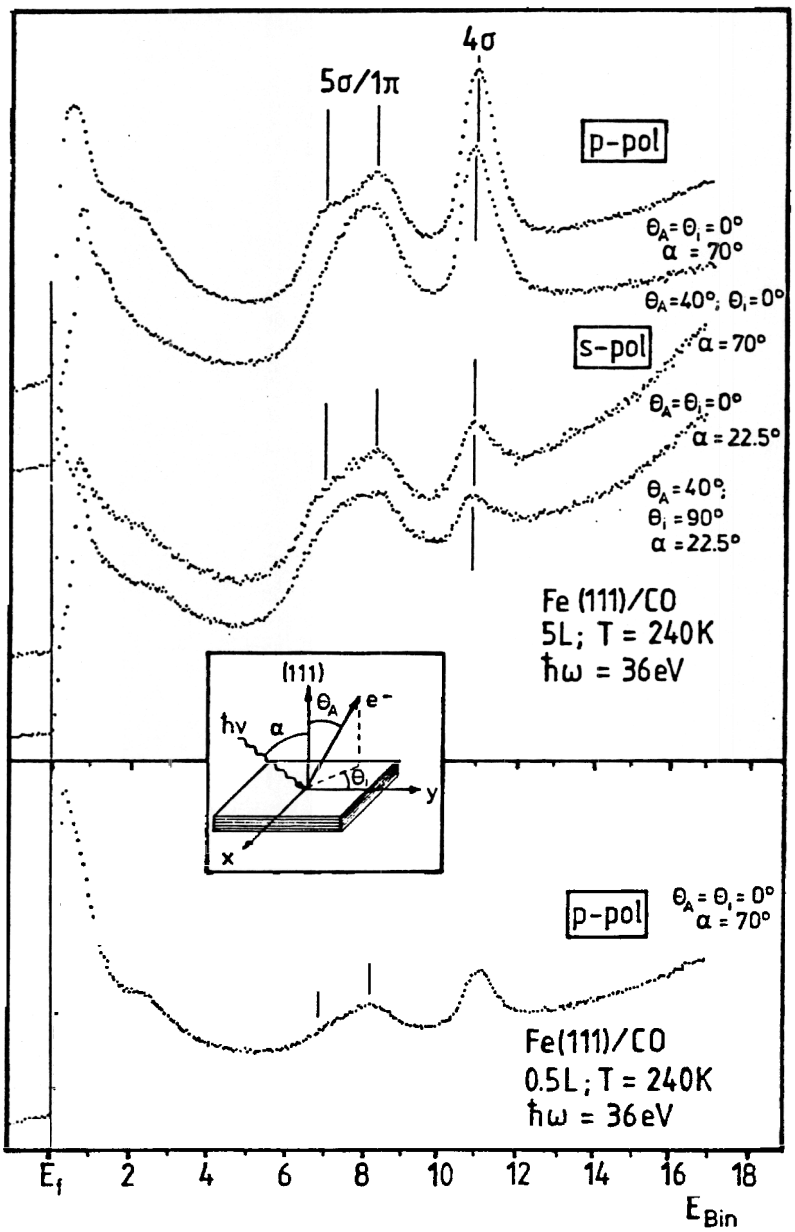


Fig. 9. ARUP-spectra of CO/Fe(111) for various light incidence and electron emission angles as indicated in the inset ($E_{Bin}$ in eV). Top and bottom panels differ by the CO exposure. The top panel corresponds to saturation coverage (ref. 66).

2.1.2 CO

As documented in the previous section the adsorption of CO has been extensively investigated with ARUPS. The orientation of the CO molecule has been found to be parallel to the surface in the case of Ag(111) (ref. 10), and upright in many chemisorbed systems (refs. 24-40). Recently, some systems have been studied where CO shows photoemission patterns different from the usual behaviour. Fig.9 presents spectra for CO/Fe(111) (ref. 66). The 5σ/1π-band is clearly split, and the 4σ intensity is not

completely attenuated in the forbidden geometry indicating a possible tilt of the CO molecules or a strong distortion of the 4σ wavefunction. Spectra have been reported for CO/Cr(110) (ref. 29) and CO/Fe(100) (refs. 67) where the authors claim flat lying CO. These are the only cases where strongly chemisorbed CO appears to be oriented parallel to the surface.

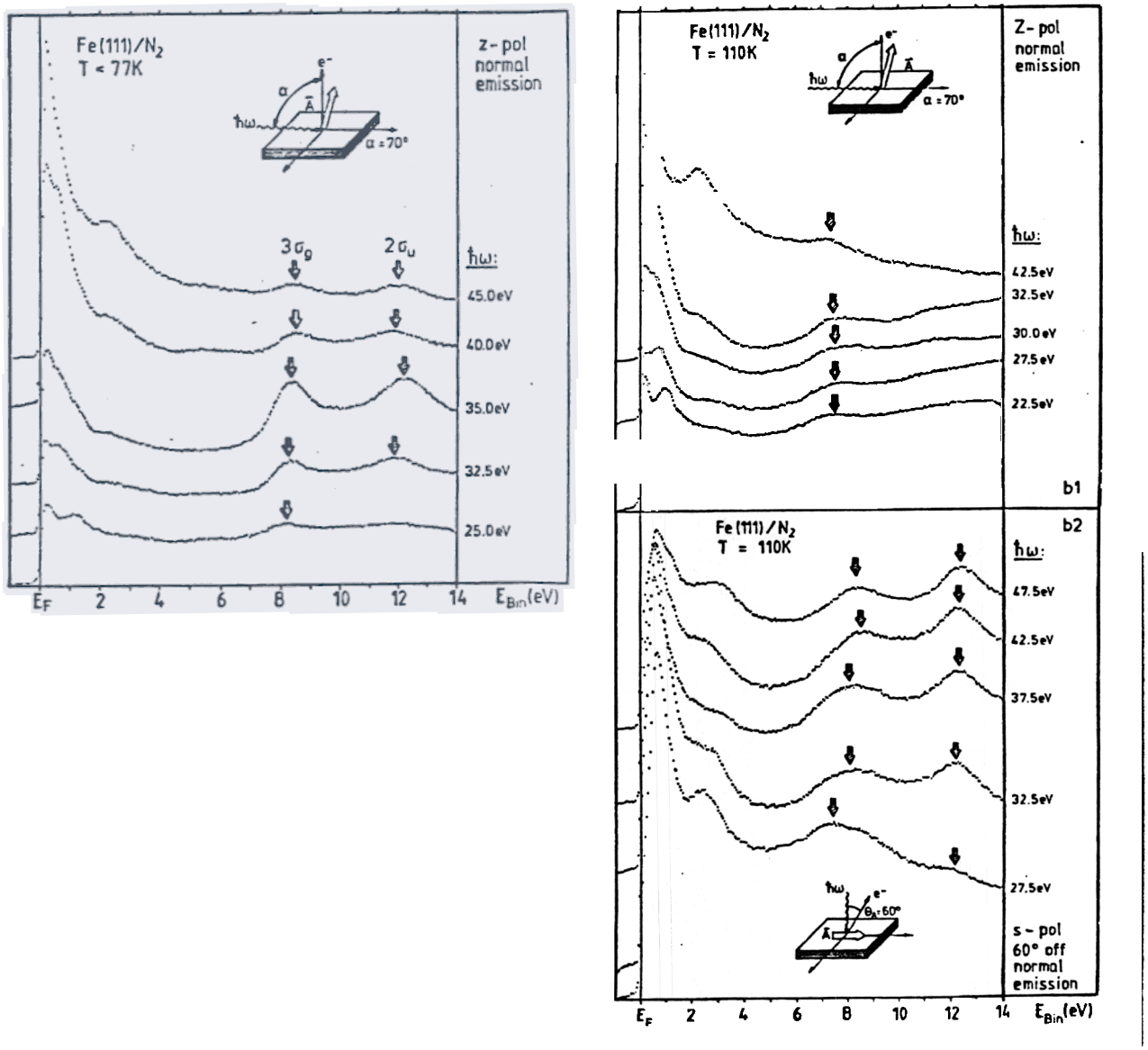


Fig. 10. ARUP-spectra of $N_2$/Fe(111) for grazing light incidence and normal emission (left panel), and s-polarization (near normal incidence, right panel) and two electron emission angles (b1: normal emission; b2: off-normal(60°) emission). For each measurement geometry typical spectra at different photon energies are plotted (ref. 72).

### 2.1.3 $N_2$

$N_2$ on Fe(111) has been the model system to investigate the mechanism of ammonia synthesis (ref. 68). It is known that $N_2$ dissociation is the rate limiting step, and that there exist molecular precursor states for dissociation where $N_2$ has been presumed to be side-on bonded to the iron surface (ref. 69). Via ARUPS a strongly inclined $N_2$ species was identified (ref. 70) in addition to a vertically bound $N_2$ species which only exists at lower temperature. Fig.10 shows a set of angle resolved spectra at low temperature (vertically bound $N_2$) and higher (T=110K) temperature ($N_2$ bound inclined). Fig.10a reveals the σ-shape resonance in normal emission for z-polarized light at T<77K. Fig.10b shows a σ resonance, but only in off-normal emission for s-polarized light (compare left and right part of this figure) at T=110K, supporting the proposed inclined geometry in the second case. A more detailed discussion including the theoretical aspects of the two $N_2$ bonding modes is given in ref.70. Another interesting feature can be demonstrated on the basis of the present results. Both, the $3\sigma_g$ as well as the $2\sigma_u$ state exhibit the shape resonance behaviour, while in the gas phase the $\sigma_g$ resonance is symmetry forbidden. The reason is very simple: The inversion symmetry of the homonuclear $N_2$ molecule is broken upon adsorption which makes the final resonance state accessible to both σ states. This was demonstrated earlier by Horn et al. (ref. 71) for the system $N_2$/Ni(110). In contrast to the case $N_2$/Fe(111) where $N_2$ dissociates at low temperature (T>140 K), $N_2$-metal coupling is usually rather weak (refs. 34, 71-74). This leads to the existence of rather intense shake up structure as noted for several $N_2$-transition metal systems (refs. 34,71-76). The experimental findings are corroborated by several theoretical calculations (refs. 34, 71-76).

### 2.1.4 $O_2$

Only a small number of ARUPS studies have been reported on molecular $O_2$ adsorption, which is probably due to the relatively high reactivity of the system leading to dissociative adsorption. A prominent example for molecular adsorption is the system $O_2$/Ag(110) (ref. 77) where at T~20 K $O_2$ was found to be physisorbed, and even more interesting a chemisorbed $O_2$ dissociation precursor state has been detected below 170 K. Only for $O_2$/Pt(111) (refs. 78-79) similar conclusions have been

reached. Whether the chemisorbed $O_2$ species must be looked at as an open-shell $O_2$ or a closed shell peroxo-species appears to be the interesting question.

### 2.1.5 CN

Very recently Conrad, Bradshaw and coworkers (ref. 80), and Netzer et al. (ref. 81) published ARUP-spectra of adsorbed CN. The adsorbate was prepared by decomposition of $(CN)_2$ as previously reported (ref. 82). The analysis reveals that CN must be adsorbed parallel to the surface plane, and that the species is basically a CN-anion. For example, the $4\sigma$ intensity is weak in normal emission which must be expected for a flat lying molecule. Since $CN^-$ is isoelectronic with CO and $N_2$ one would have expected a similar adsorption geometry for CN, i.e perpendicular to the surface. The theoretical studies published so far (refs. 83-84) assume a linear metal CN bond geometry. These calculations reveal that $2\pi$ back donation plays a minor role in CN bonding which is due to the relatively high energy of the antibonding $2\pi$ level. This is expected because the electron affinity of a CN-anion is very low. Thus one of the prerequisites for linear molecule-metal bonding according to the $\sigma$-donation-$\pi$-back-donation model is missing, which leads to the flat bonding geometry found experimentally.

### 2.1.6 NO

Although NO has been studied for a long time with various methods (ref. 85) only very few ARUPS studies (refs. 86-88) have been published. The axis of the NO molecule appears to be oriented parallel to the surface normal in the case of the c(4x2)NO/Ni(111) (ref. 87) system but not in all cases. This corresponds to the bonding geometry known from NO-transition metal complexes (ref. 89). There are basically two bonding modes known for NO, the nature of which depends on the charge transfer between the molecule and the surface. Two extreme cases are considered: i) $NO^+$, which is isoelectronic with CO, and thus exhibits similar bonding characteristics, ii) neutral NO, which has an additional electron in the $2\pi^*$ level, leading to a weakening of the metal-NO bond and a bent metal molecule complex.

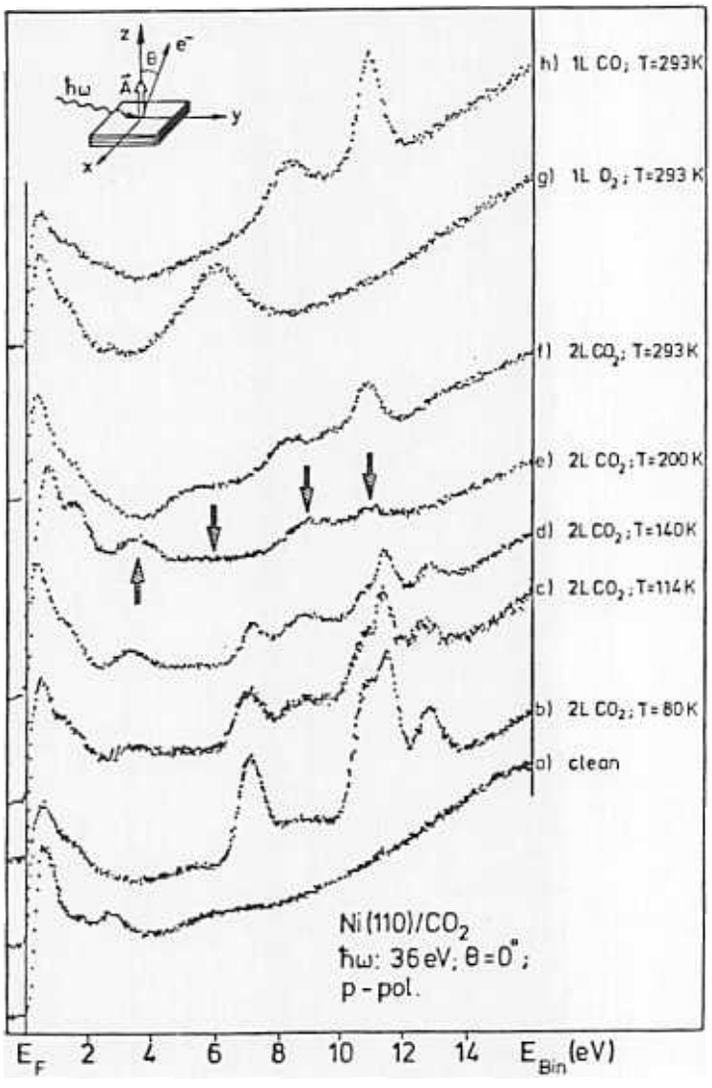
z
θ
e⁻
ħω
A
y
x
h) 1L CO; T=293K
g) 1L O2; T=293 K
f) 2L CO2; T=293K
e) 2L CO2; T=200K
d) 2L CO2; T=140K
c) 2L CO2; T=114K
b) 2L CO2; T=80K
a) clean
Ni(110)/CO2
ħω: 36eV; θ=0°;
p-pol.
E_F
2
4
6
8
10
12
14
E_Bin (eV)

chemisorbed species is found which shows three features marked with arrows. One additional feature around 5eV (see arrow) is forbidden in normal emission indicating $C_{2v}$ symmetry of the adsorption site. Comparison with results of cluster calculations (ref. 96) shows that this is a bent anionic $CO_2^-$ species. Whether the $CO_2^-$ species is carbon or oxygen bound to the surface cannot be decided on the basis of the present results. Above 200K (spectrum f)) this species dissociates into CO and O, both adsorbed on the surface, as is clear from a comparison with the spectra of pure CO and O adsorbates (spectra g)-h)). It was concluded from this study that $CO_2^-$ is an intrinsic precursor for $CO_2$ dissociation. Note that $CO_2^-$ is isoelectronic and isostructural to $NO_2$, which is known to dissociate rapidly upon adsorption also at low temperature (ref. 91). $CO_2$ is known to react on Ag(110) surfaces with co-adsorbed oxygen to form a carbonate $CO_3$ species. ARUPS has been employed (refs. 97-98) to study the $CO_3$ orientation. It is found that $CO_3$ assumes an orientation with $C_s$ symmetry and the plane along the (110) direction a mirror plane.

2.1.8 $HCOO^-$

The adsorption of formic acid often leads to the formation of formate anions. Recently, several groups have studied the adsorption of $HCO_2^-$ on Cu(110) with ARUPS (refs. 99-100). Fig. 12 taken from the work of Hofmann and Menzel (ref. 99) shows a set of ARUP-spectra of this system for various orientations of light polarization relative to the Cu(110) surface azimuths, but all taken in normal emission. For normal emission the selection rules are particularly simple, because the final electron state $\Phi_e$ in the present case belongs to the representation $a_1$ in $C_{2v}$. The x,y,z-components of the dipole operator transform like $b_1$, $b_2$, and $a_1$, respectively. Since the light always impinges under a finite angle ($\alpha$=20°;small z-component and 65°;large z-component), there is always a z component, but $b_1$ and $b_2$ are selected by going from the (110) to the (001) azimuth. Therefore, $b_1$ and $b_2$ initial states can be selected in the two azimuths. Comparing spectra a and b we identify $b_1$ derived levels at 4.8 eV and 9.5 eV, and a $b_2$ derived level at 7.7 eV. Increasing the z-component in spectra c and d shows $a_1$ derived levels at 5.0eV, 9.7 eV, and 13 eV. The $a_2$ level indicated on the basis of theoretical calculations (ref. 101) is dipole

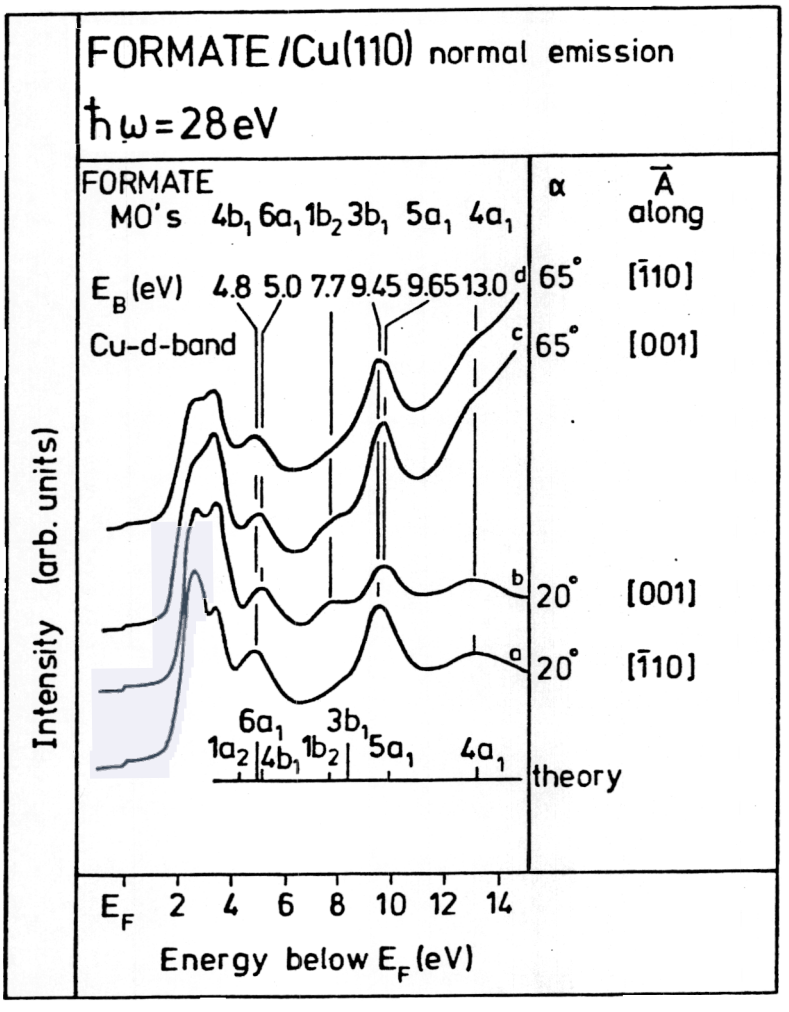


Fig. 12. ARUP-normal-emission-spectra as a function of light polarization for $HCO_2^-$/Cu(110) (ref. 99). Explanation see text.

ingredient to understand $H_2O$ adsorption, and has been postulated in almost all studied $H_2O$ adsorption systems.

### 2.1.10 $NH_3$

Ammonia adsorption (refs. 105-107) represents one of the few molecular adsorption systems where azimuthal angle distribution patterns (ref. 105) were used to try to unravel molecular orientation. Fig.13 shows azimuthal patterns from the $NH_3$ 1e level, 11.3 eV below the Fermi energy. The detector was

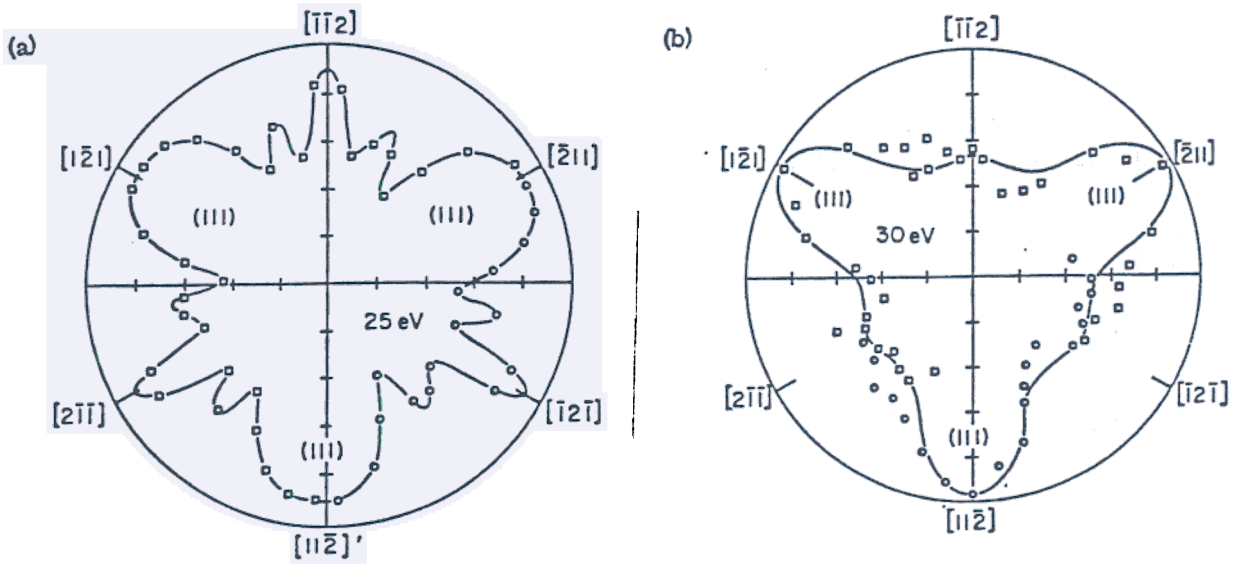


Fig. 13. Azimuthal variations of the off-normal (42-45°) emission intensity of the 1e emission of $NH_3$/Ir(111) at two different photon energies. The data have been measured for a 120° azimuthal sector (circles), and then symmetrized to 360° (squares) (ref. 105).

positioned off-normal (42-45°), and the sample was rotated about the surface normal. Light impinges at 45°. The observed intensity of the 1e level is recorded and plotted in Fig.13. It is clear that the three N-H bonds of the $NH_3$ molecules must be locked into one fixed orientation on the surface. By comparison with theoretical calculations (ref. 108) it was concluded that the exact orientation of $NH_3$ could not be derived from the experimental data.

### 2.1.11 Hydrocarbons

Acetylene (ref. 109), ethylene (refs. 109-111), and benzene (refs. 112-119) adsorption have been studied extensively in the past. As is obvious from the above discussion ARUPS is particularly useful if the symmetry of the adsorbate site is

reasonably high, so that selection rules can be defined. For hydrocarbons this is not always the case. As an example, where the selection rules can be applied favourably, we consider here a series of studies on benzene adsorption published by Netzer and collaborators (refs. 113-118). It was deduced that on the group VIII transition metals (Ni,Pd,Pt,Rh) benzene adsorbs basically unperturbed in $C_{6v}$ symmetry with surface bonding occurring through the π-electrons of the intact aromatic ring. On other transition metals the aromatic ring appears to be distorted, for example on Os(0001) (ref. 116), as was shown via ARUPS. On Os(0001) $C_6H_6$ undergoes chemical reactions as a function of temperature, finally forming hydrocarbon fragments on the surface. ARUPS (ref. 119) indicates that before the carbon ring is cracked precursor states are populated on the surface. One of these precursor states is proposed to be a aryne-like $C_6H_4$ species with a carbon ring system oriented by about 45° inclined with respect to the surface normal (ref. 119). Preferential azimuthal orientation of benzene molecules on Rh(111) has been reported (ref. 120). On Pd(111) ARUPS has been used to study the low temperature formation of benzene via cyclotrimerization of $C_2H_2$ (refs. 121-122). The spectra of the benzene formed did not show the typical shift of the π-electron states known from chemisorbed $C_6H_6$ (refs. 112-120). This was attributed to the co-adsorption of the reacted acetylene.

Very recently, the adsorption and orientation of large aromatic molecules like anthracene and tetracene has been studied by Koch and his group via ARUPS (ref. 123). The remarkable intensity variations between σ and π electrons, oriented in and out of plane of the aromatic ring plane, observed in these cases are documented in Fig. 14 for tetracene. The spectra indicate that the tetracene plane is oriented perpendicular to the surface plane.

## 2.2 Co-adsorbates

ARUPS has been used in the past, and will be even more frequently employed in the future, to investigate the electronic structure of co-adsorbates.

The adsorption of atomic hydrogen induces marked changes in the electronic structure of co-adsorbed CO on Ni(100), as was recently shown with ARUPS by Bradshaw and his group (ref. 124). This is shown in Fig. 15 where spectra of a pure CO (a), a H+CO

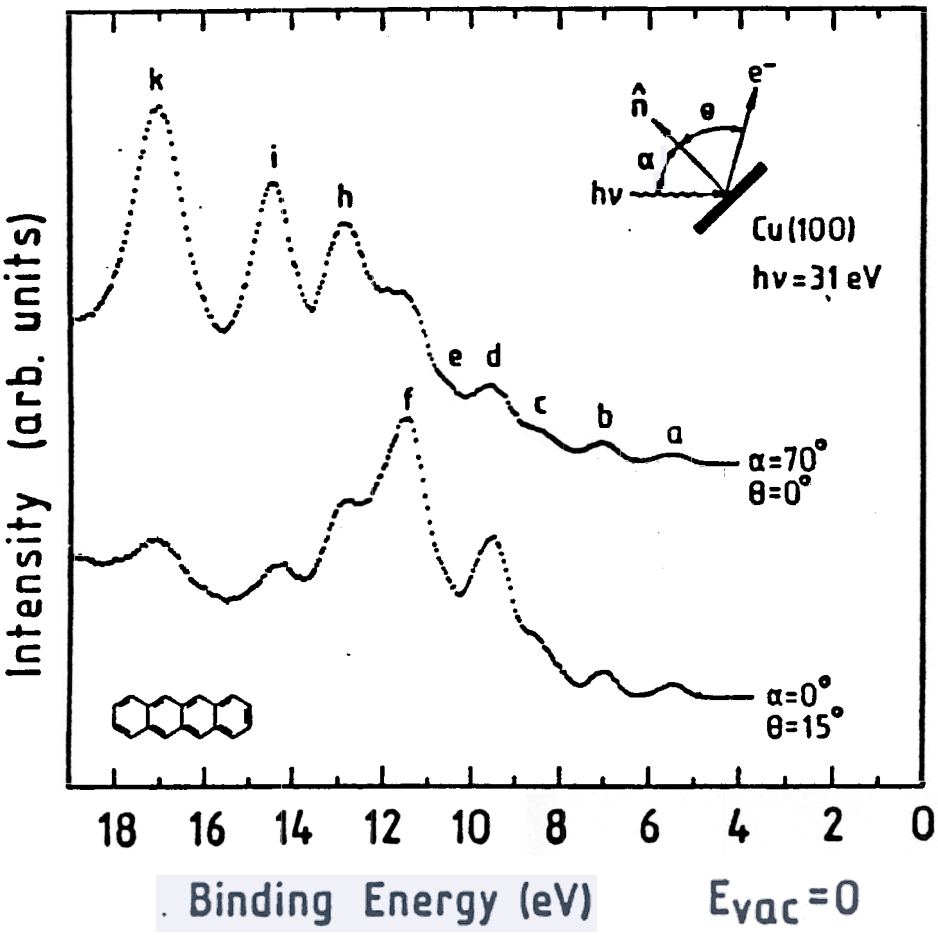


Fig. 14. ARUP-spectra of a tetracene/Cu(100) adsorbate in two measurement geometries as indicated (ref. 123).

adsorbate, with both gases exposed to saturation coverage (b), and a H+CO adsorbate, so called Σ-state (c), where the hydrogen coverage is lower than in case (b) are shown. The spectra are taken with polarized synchrotron radiation in the forbidden geometry. In spectra (a) and (b) we find the normal behaviour documented in Fig.5. This is typical for CO molecules oriented perpendicular to the surface plane. In spectrum (c), however, the emission intensity of the 4σ state is not suppressed, which is consistent with a slightly tilted bonding geometry or a strong distortion of the 4σ ion state wavefunction. Also, the normal emission spectra with z-polarization are different from a pure CO adsorbate, and there are indications of weak satellite structure on the high binding energy side of the 4σ ionization. This is in line with the finding that the adsorption energy (ref. 125) of the Σ-state of CO+H/Ni(100) is considerably weaker as compared to CO/Ni(100), and is similar to CO/Cu(100) (ref. 126), where we expect intense satellite structure similar to CO/Cu(111) (ref. 11) discussed

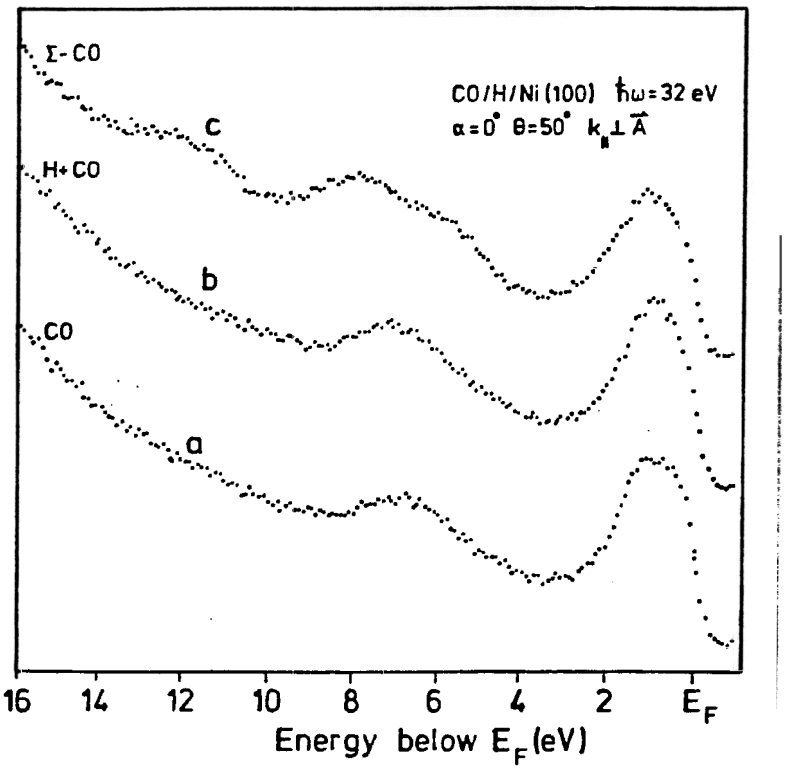


Fig. 15. ARUP-spectra of CO-, and CO+H-co-adsorbates on Ni(100) taken in the "forbidden" geometry (ref. 124).

above.

CO-alkali-co-adsorbates (ref. 127) are the most frequently tackled co-adsorbate systems with ARUPS. Several different metal surfaces have been studied (ref. 127). The most complete sets of ARUP-spectra exist for Ru(001) and Cu(100) surfaces (refs. 128-134. Some important conclusions have been drawn from these studies which were partially in contrast to existing models of CO-alkali interaction at the time (ref. 127). As monitored by the angular distribution pattern and the peaking of the shape-resonance the CO orientation with respect to the surface normal does not change upon alkali-CO-adsorption independent of alkali-coverage, except for a thick alkali film (refs. 128-134). In the case of the alkali-CO-co-adsorbates on Cu surfaces (ref. 129), interesting variations in the shake up structure have been observed by Heskett and Plummer (ref. 129) as shown in Fig.16, where both the pure CO and the co-adsorbate spectra are presented for comparison. As outlined above, the decrease of the satellite intensity can be a sign of stronger or weaker metal-CO coupling. Since, however, there are still only two CO bands we must conclude that the metal-CO-bond strength actually increases. In addition to this variation of the CO-metal bond

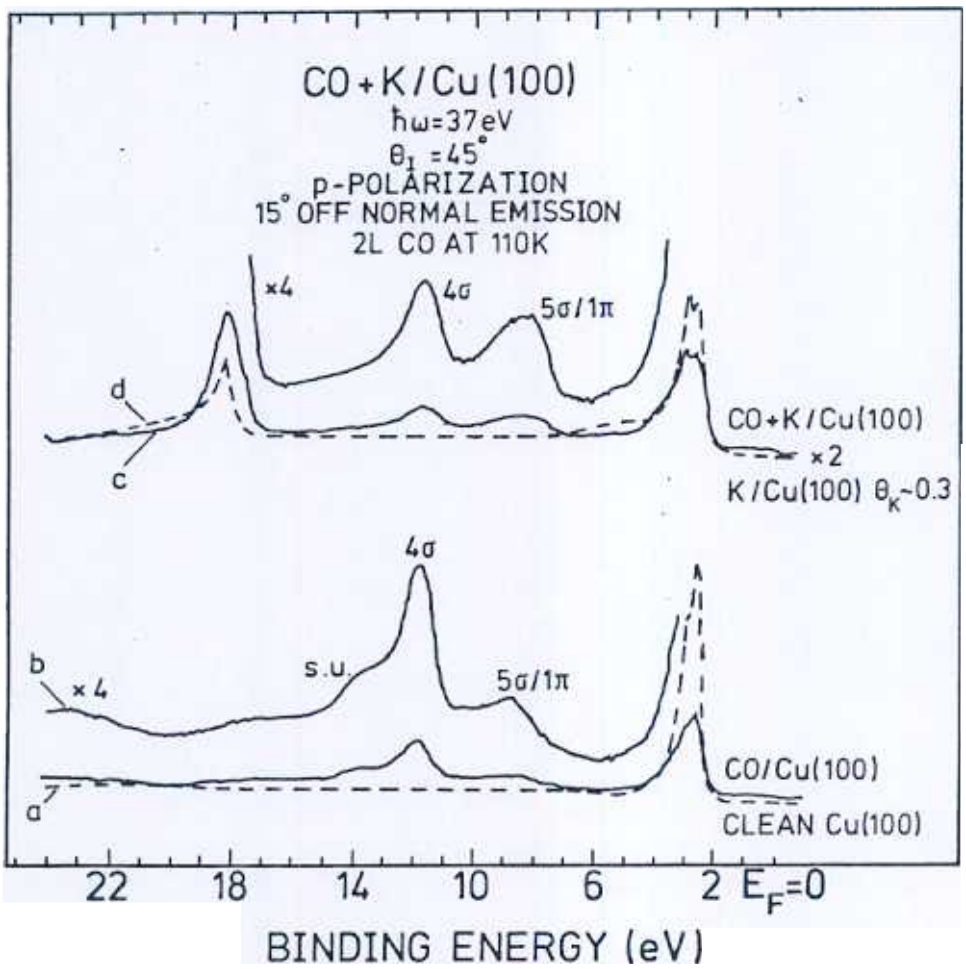


Fig. 16. ARUP-spectra for CO/Cu(100) ($\theta_{CO}$=0.5, curves b and c), and CO+K/Cu(100) ($\theta_K$=0.3,$\theta_{CO}$=0.3) in comparison. The spectra of the systems before CO adsorption (curves a and d) are shown as broken lines. The peak around 18 eV is due to K3p emissions (ref. 129). CO induced peaks are marked. The spectra were taken for light incidence angle $\theta_I$=45° and 15° off-normal emission.

strength direct CO-alkali short range interactions involving the alkali-s- and the CO-1π-orbitals have been postulated (ref. 128). Fig.17 shows two sets of spectra, one for the pure CO adsorbate, equivalent to Fig.5, and another one for the alkali-co-adsorbate. The spectra in the so called "allowed" geometry are fairly similar, but in the "forbidden" geometry they are substantially different. The 1π peaks in spectra b and c are located at different energies and the 4σ peak for CO/K has more residual intensity than expected for an unperturbed, perpendicularly adsorbed CO molecule. The shift of the 1π level in the CO/K-system to lower binding energy is similar to that observed on Pt(111) (ref. 135) or on Fe(110) (ref. 136). The fact that σ states are visible in the "forbidden" geometry may be caused by a slight tilting of the CO molecule or be due to

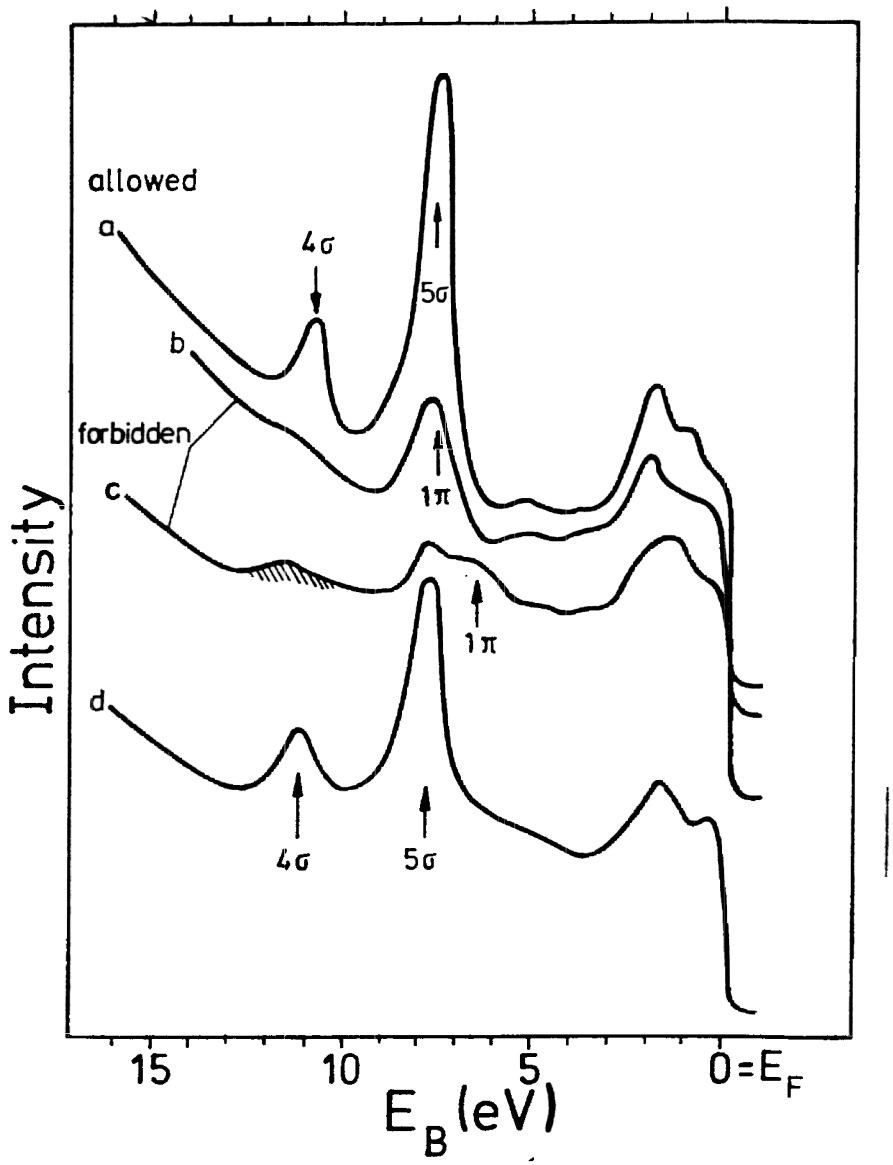


Fig. 17. ARUP-spectra in "allowed" and "forbidden" geometry (20° off-normal) for CO/Ru(001) and CO+K/Ru(001) ($\Theta_K$=0.33) (ref. 128).

the immediate vicinity of the K species, such that the symmetry of the coadsorbed CO molecule is broken. The spectra of the K/CO system are interestingly similar to those of systems like CO/Fe(111) (ref. 66). This may mean that in the latter case similar interactions, i.e. between the CO 1π and the metal surface are active. Very often alkali co-adsorption leads to stronger molecule-surface interactions (ref. 127), but there are cases where the opposite effect is observed. For example, small amounts of alkali precoverages lead to a very strong repulsive interactions with $N_2$ and attenuates $N_2$ adsorption by a factor of 4 while the electronic structure of the adsorbed $N_2$

appears to be the same as without alkali precoverage (ref. 135). ARUPS was used to prove this (ref. 137), and it has been interpreted as an indication for long range alkali-$N_2$ repulsion. Tentatively, a lack of d-π-backdonation in the case of $N_2$-transition metal bonding has been argued to be the reason for this behaviour (ref. 137).

Many other alkali co-adsorbates have been studied using photoelectron spectrosopy (ref. 127). A use of angular resolution, on the other hand, has been rather scarce in these cases. ARUPS has been used recently to study the interaction of $CO_2$ and alkali co-adsorbates (ref. 138), benzene with alkali-co-adsorbates (ref. 139) on transition metals, and CN-alkali co-adsorbates (ref. 140). $CO_2$ dissociates into CO and O at very low temperatures ($T<110$ K) when Pd(111), for example, is predosed with Na (ref. 138). On clean Pd(111), on the other hand, $CO_2$ does not adsorb. On thick alkali metal films different $CO_2$ reaction channels, i.e. towards the formation of $CO_3$ are opened (ref. 138). The CN-alkali co-adsorbates (ref. 140) are interesting because they allow direct comparison of the photoemission characteristics with bulk cyanide salts (ref. 141). It is clear that an ionic phase is formed on the surface (ref. 140).

Interesting results have been obtained on mixed $N_2$ and rare gas atom layers at low temperatures by Umbach, Menzel and collaborators (ref. 74). A monolayer of $N_2$ on Ni(111) consists of two states one of which is chemisorbed and vertically bound to the surface, while the other is physisorbed and probably lies flat on the substrate between the chemisorbed molecules. If such a layer is exposed to Ar, the physisorbed $N_2$ layer is replaced.

Research activities on co-adsorbates involving electronegative co-adsorbed species, like oxygen or halogens have been much less intense. There are several reports on photoelectron spectroscopic studies but only a few ARUPS studies have been reported (ref. 142-143). Again the influence of oxygen co-adsorption on CO-Cu-adsorbates has been studied under the aspect of studying the influence on satellite intensities and absorption geometries (ref. 142). These studies point to specific CO-O interactions or oxygen induced variations in the CO-metal interaction. In other cases like CO+O on Pd(111) the

experimentally found results can be understood without considering CO-O interactions (ref. 143).

## 3. INTERMOLECULAR INTERACTIONS IN ORDERED OVERLAYERS

Intermolecular interactions are always present in real adsorbate systems. Intermolecular interactions determine among other things the chemical reactivity between adsorbed species and also the ordering of the adsorbed overlayers. The present section is dedicated to cover this latter aspect because ordering leads to a two dimensionally periodic arrangement of adsorbed particles. As mentioned in the introduction and illustrated in Fig.1 we can assign a certain space group to this arrangement, and then classify the electronic band states of the system according to the space group. Experimentally, molecular band dispersions were first observed by Horn et al. (refs. 31, 144) for CO overlayers, and interpreted in terms of tight-binding calculations (refs. 31,145) on free unsupported two dimensional CO arrangements.

### 3.1 Pure adsorbates

As an introduction to the quasi two dimensional band structure of molecular overlayers we discuss the band dispersions and the symmetry properties of a hexagonal overlayer (ref. 27) of CO molecules on a fcc(111) surface as shown in Fig.1. If the intermolecular interaction potential is large enough to demand consideration of the two-dimensional crystal periodicity, the overlap of adsorbate wavefunctions is sufficient to produce two-dimensional Bloch states $\Psi_k$ and to make a band description of the electronic structure more appropriate. Then the wave function at a lattice site $R_1$ is related to the wave function at site $R_2$ by:

$$\Psi_k(R_1) = \exp[ik(R_1-R_2)]\Psi_k(R_2) \qquad (3)$$

where $\exp[ik(R_1-R_2)]$ gives the phase difference between the two sites for a state specified by the two-dimensional wave vector k. Before we consider the changes in the band structure introduced by the substrate we will briefly discuss the qualitative behaviour of the band dispersion of a hypothetical support free molecular layer (ref. 145) as shown on the left of Fig.1. We can illustrate the qualitative features of the dispersion by plotting schematically the real parts of a tight-binding wave function in real space for values of k

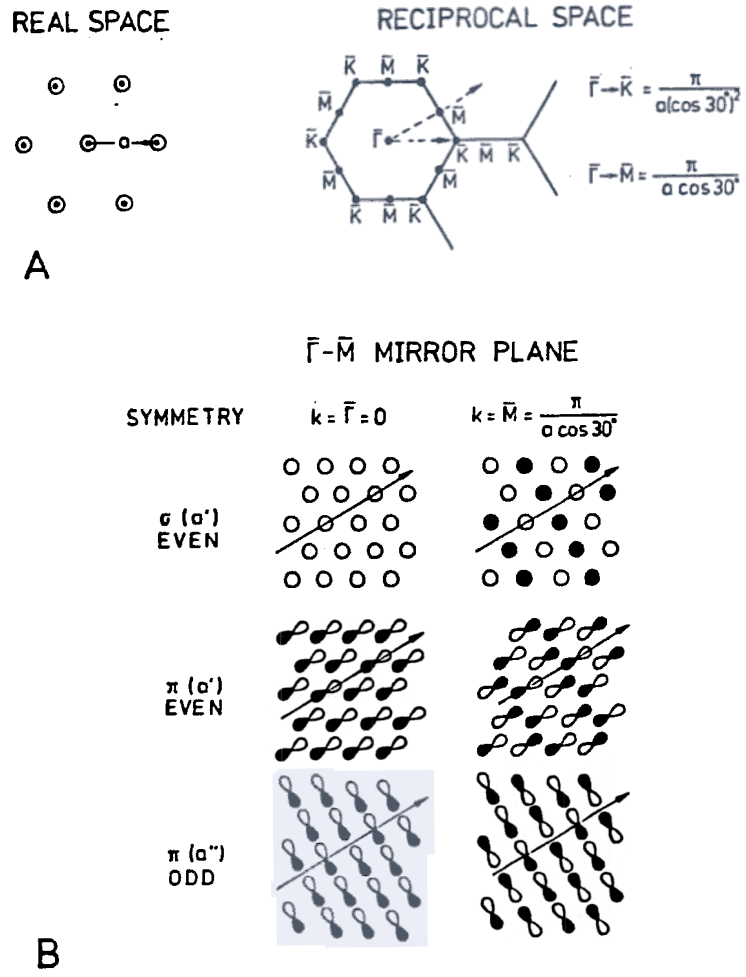


Fig. 18. (a) Schematic representation of the real and reciprocal space structures of a hexagonal (√3x√3)R30° CO overlayer. (b) Schematic representation of a two-dimensional σ- wavefunction and two two-dimensional π-wavefunctions at two points of high symmetry in the Surface Brillouin Zone (ref. 27).

corresponding to high symmetry points in reciprocal space. Fig.18a shows the real- and reciprocal-space unit cells for the hexagonal structure. The real and reciprocal lattices have two mirror planes, one along the $\bar{\Gamma}$-$\bar{M}$-$\bar{\Gamma}$ line (in reciprocal space), and the other one along the line $\bar{\Gamma}$-$\bar{K}$-$\bar{M}$-$\bar{K}$. The wave functions along these lines will be even (a') or odd (a''). Fig.18b illustrates the phases of a σ and the two π states at $\bar{\Gamma}$ and $\bar{M}$. At $\bar{\Gamma}$ (k=0) all the wave functions at the different lattice sites are in phase. This results in a strongly bonding configuration for the σ state (top row), but an anti-bonding configuration for both π states because the individual π functions change sign about the molecular axis. The π functions have been chosen so that one is even and one is odd with respect to the mirror plane. Because at $\bar{\Gamma}$ the wave functions transform according to

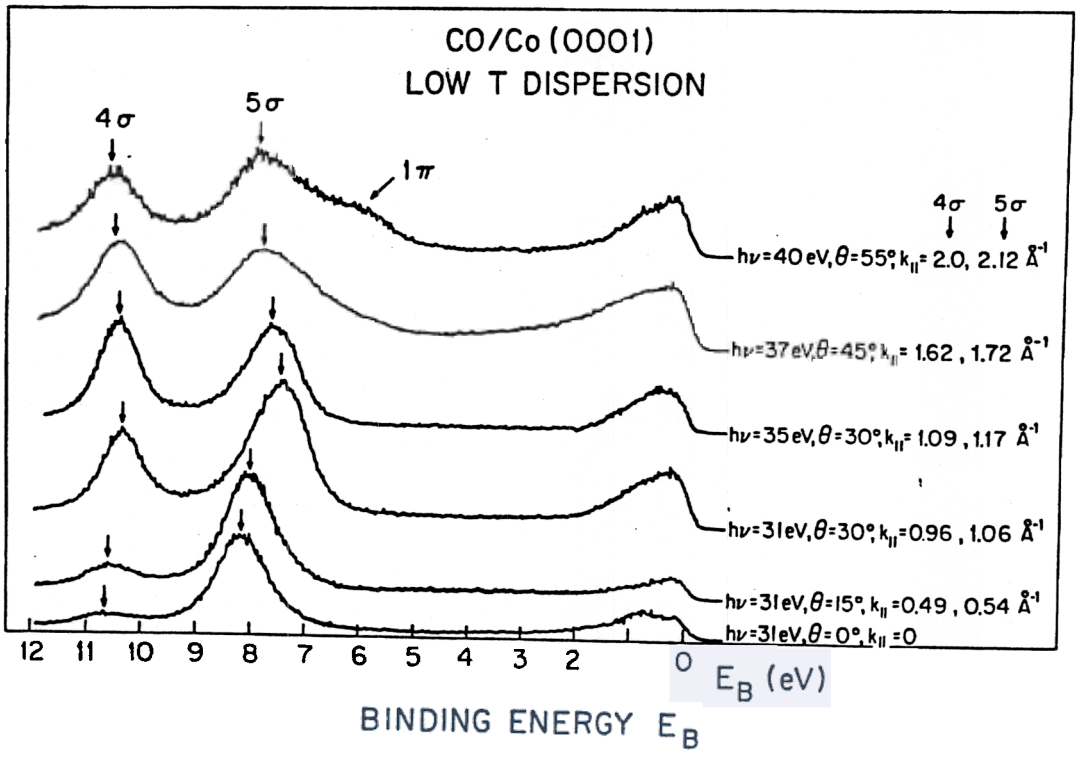


Fig. 19. ARUP-spectra of a $(2\sqrt{3}x2\sqrt{3})R30°$ CO overlayer on Co(0001) for different values of the two-dimensional wave vector $k_{\parallel}$ as indicated in the figure. The positions of the CO induced features are marked with arrows (ref. 27).

$C_{6v}$, the two π components are degenerate. Therefore, at $\bar{\Gamma}$ we have a strong bonding σ band and a degenerate antibonding π band. Along the mirror plane k increases from 0 at $\bar{\Gamma}$ to π/(acos30°) at the zone boundary $\bar{M}$. The second column shows the wave functions at $\bar{M}$ where the arrow indicates the direction of k. All rows of atoms parallel to k have the same phase but each row has a phase change of π. The result for the σ states is that each atom is surrounded by four atoms of opposite phase (antibonding) and two bonding atoms. The σ bands therefore disperse upward from $\bar{\Gamma}$ to $\bar{M}$. In contrast, the even π state is strongly bonding since each lobe of the molecular π orbitals sees only bonding nearest neighbours. The even π band disperses downward from $\bar{\Gamma}$ to $\bar{M}$ with the largest difference in the π band energy. The odd π state at $\bar{M}$ is just slightly more bonding than the π state at $\bar{\Gamma}$ since the overlap of the lobes in a line perpendicular to k is antibonding but the overlap between the lines of atoms is bonding. This means that at $\bar{M}$ the two π derived bands are no longer degenerate as a consequence of the lower symmetry of the $\bar{M}$ point. Thus we have explained the qualitative features of the dispersions in the $\bar{\Gamma}$ to $\bar{M}$ direction shown in Fig.1. Analogously the dispersions in the other

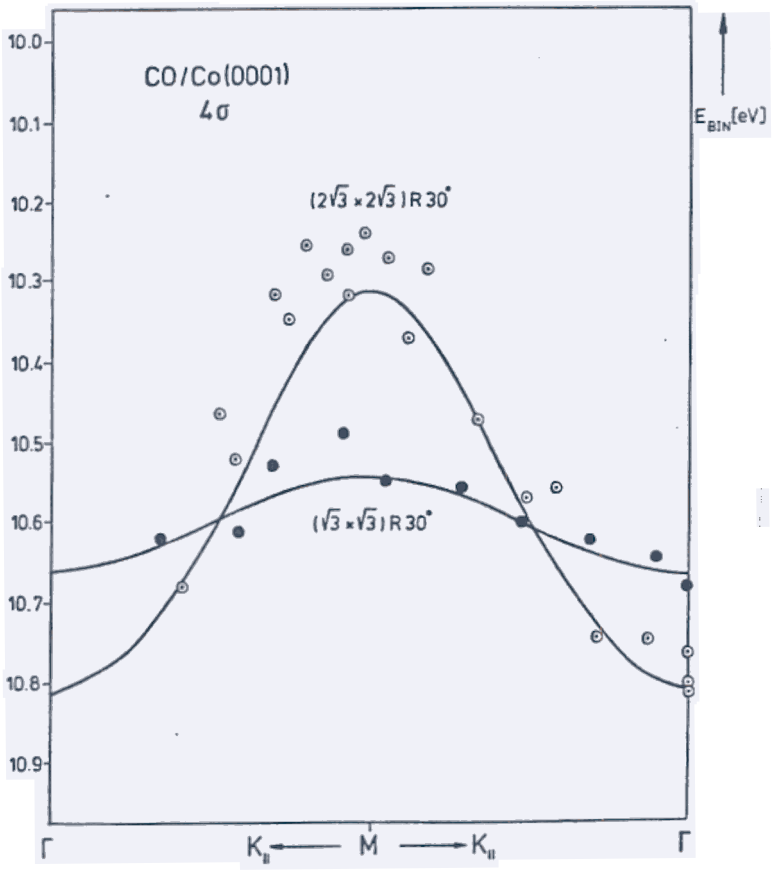


Fig. 20. Measured (circles) and calculated (full lines) $k_{\parallel}$ dispersions of the 4σ level in two hexagonal CO overlayers on Co(0001). Filled circles refer to the (√3x√3)R30° structure, open circles to the (2√3x2√3)R30° structure (ref. 27).

directions of high symmetry in the Surface Brillouin Zone can be explained, and we refer to the literature for a more detailed discussion (ref. 27).

Such dispersions can be determined via ARUPS as shown in Fig.19, where spectra of a (2√3 x 2√3)R30° CO/Co(0001) overlayer for different values of the wave vector k are plotted. The wave vector is varied by varying the photon energy and the emission angle within the direction of the considered surface azimuth as noted in the figure. The connection between k and the varied quantities is given by:

$$k_{\parallel} = (2m_e h^{-2} E_{kin})^{1/2} \sin\theta \qquad (4)$$

where $k_{\parallel}$ is the wave vector parallel to the surface, which is the conserved quantity. Fig. 20 shows a comparison of calculated dispersions for the 4σ-derived band with measured 4σ dispersions of CO/Co(0001) adsorbates in $\bar{\Gamma}$-$\bar{M}$ direction in two hexagonal (√3x√3)R30° and (2√3x2√3)R30° layers (partially based on Fig.19).

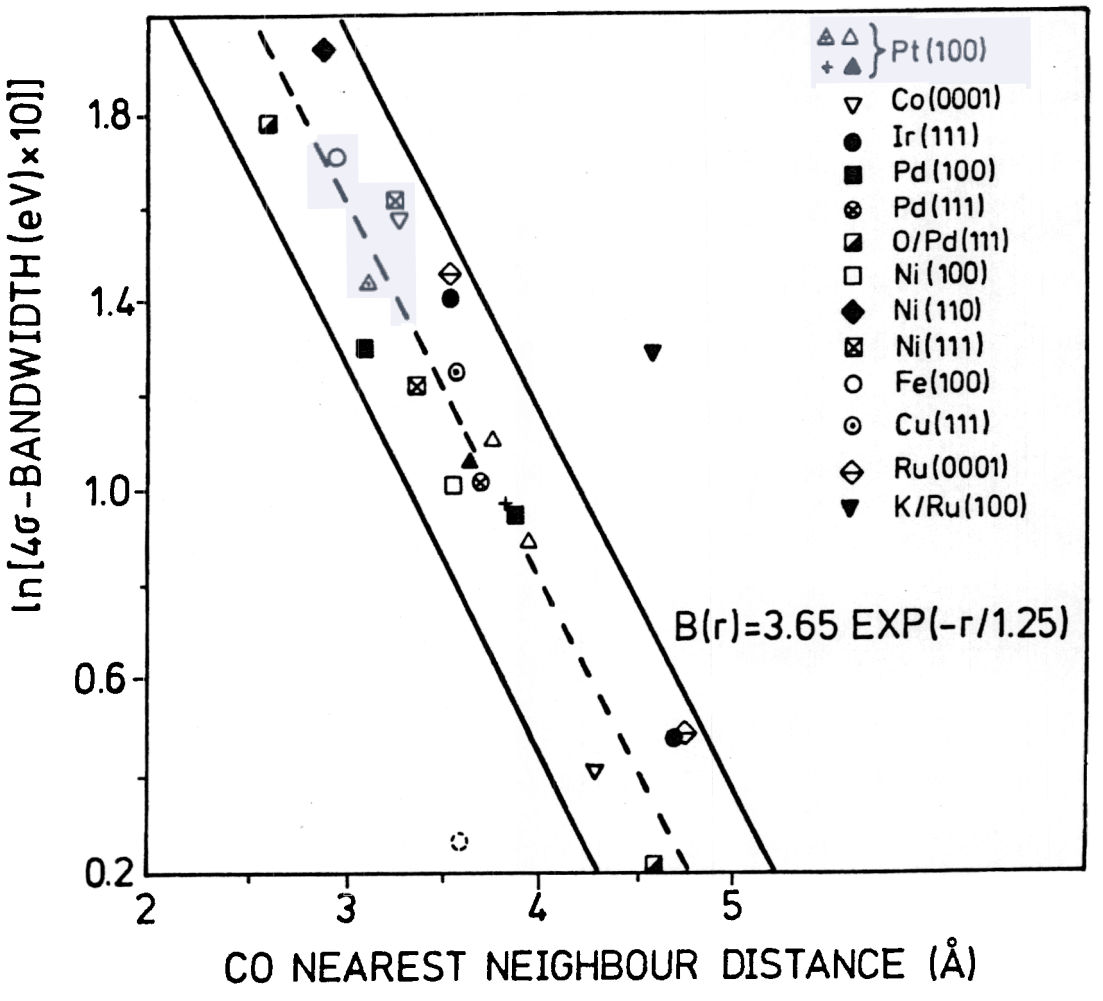


Fig. 21. Plot of the 4σ band widths of various CO overlayers as a function of the CO-CO separation (refs. 11,25-28,30-31,33-34,39,143-148). The CO-CO separation has been estimated on the basis of published structure models used to explain the observed LEED patterns.

We have artificially set the lengths of the two Brillouin zones equal for a more convenient comparison. Due to the smaller CO-CO distance in the (2√3 x 2√3)R30° layer, the overlap of the 4σ CO wave functions increase, and concommitantly, the band width increases. Fig.20 illustrates that the increase in band width can be quantitatively reproduced by simple tight binding calculations in the case of 4σ derived bands. In the present case the comparison can be made directly because the number of nearest neighbours is the same in both systems. If, on the other hand, we want to compare dispersions in hexagonal and quadratic systems, the observed band widths have to be corrected for the different number of nearest neighbours. Such a correction is straightforward on the basis of simple tight binding considerations. The result of such a comparison for several different adsorbate systems is shown in Fig.21 (refs. 11, 25-28,

30-31, 33-34, 39, 143-148). The data points follow an exponential dependence on the nearest neighbour distance with a decay length on 1.25 Å if we disregard the CO-K co-adsorbate for the moment. This strongly supports the conclusion that the 4σ dispersion is caused by direct CO-CO overlap. Intuitively, this is reasonable, because the 4σ CO level is not strongly involved in the metal substrate bonding. At the same time we expect a completely different behaviour for the 5σ level, because in this case the interaction with the substrate as indicated in the middle of Fig. 1 should have a marked influence on measured dispersion. There is no such linear dependence of the observed band width as a function of CO-CO distances as for the 4σ level (ref. 34). A similar plot as for the 4σ level exhibits no particular functional dependence, which may be an expression of the participation of indirect through substrate interactions in intermolecular interaction. Care has to be exercised not to jump to this conclusion prematurely, because, due to the stabilization of the 5σ level into the region of the 1π level (see Fig.1) we expect strong 5σ/1π hybridization effects which have to be taken into account in the prediction of band dispersions (ref. 27).

There are only very few cases, where the complete band structure in the 5σ/1π region has been determined. One such example, which shall be considered in the following, is the system CO(2x1)p2mg/Ni(110) (ref. 26). In this system the coverage is Θ=1, and the lateral stress is particularly demanding. Fig.22 shows a model of this structure. The interesting structural feature is the glide plane along the densely packed rows ((110) azimuth) of the Ni(110) surface. The unit cell of this overlayer contains two CO molecules, which leads to peculiar consequences for the ARUP-spectra. Fig.23 shows the measured dispersions and a calculated tight binding band structure for comparison. A doubling of the number of bands is found. Therefore we observe eight, instead of 3(if 1π is degenerate) or 4, features for the $\bar{\Gamma}$ point in the Surface Brillouin Zone. The eight features are classified in Fig.23 according to the wave function character of the parential molecular ion state (4σ, 5σ, 1π), and even and odd behaviour with respect to operation of the glide plane ($4\sigma^+$, $4\sigma^-$, etc.). Due to the twofold symmetry of the adsorbate, the two components of the 1π level ( $1\pi_x$, pointing along the (110) azimuth;

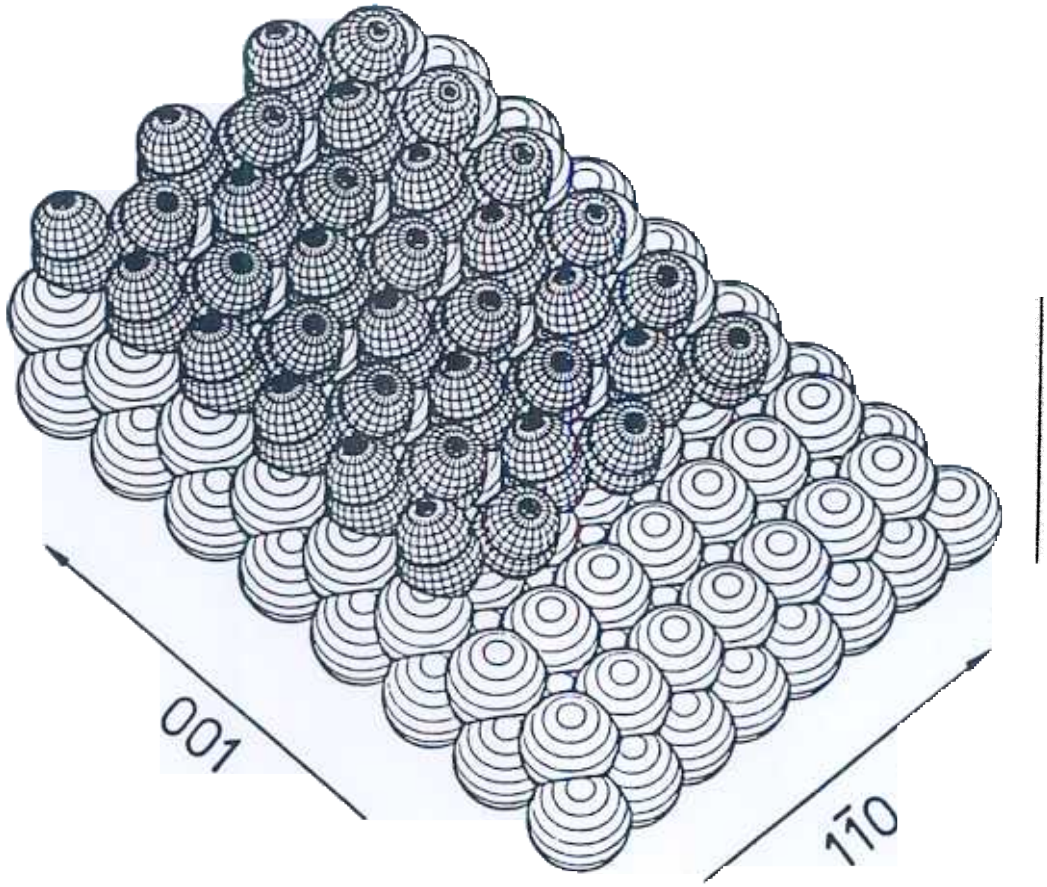


Fig. 22. Structure model of the CO(2x1)p2mg/Ni(110) adsorbate (ref. 26).

$1\pi_y$, pointing along the (100) azimuth) are not degenerate. All bands are degenerate pairwise at the X-point which is required by symmetry of the p2mg non-symmorphic space group (ref. 149). The important point is that the p2mg system allows a detailed assignment and comparison with calculations in the region of the $5\sigma/1\pi$ band system. Fig.24 shows schematic representations of the $1\pi$ and $5\sigma$ wave functions at $\bar{\Gamma}$. The two $1\pi_x$ orbitals in the unit cell interact strongly due to the short distance along the (110) azimuth and split by more than 2 eV. The $1\pi_y$ orbitals interact much less strongly and split only by 0.7 eV. The $5\sigma$ orbitals split by more than 1 eV. Without the theoretical calculation one is trying to determine the $5\sigma$ band width by taking the splitting between the $5\sigma^+$ and the $1\pi_x^-$ bands which is only 0.6 eV. The observed band dispersion is caused by hybridization of the crossing $1\pi_x^-$ and the $5\sigma^+$ bands, which along $\bar{\Sigma}$ belong to the same irreducible representation in the p2mg space group. The values used to correlate $5\sigma$ band widths versus CO-CO distance as mentioned above have been determined without detailed knowledge of $5\sigma/1\pi$ hybridization. Therefore we reach the conclusion

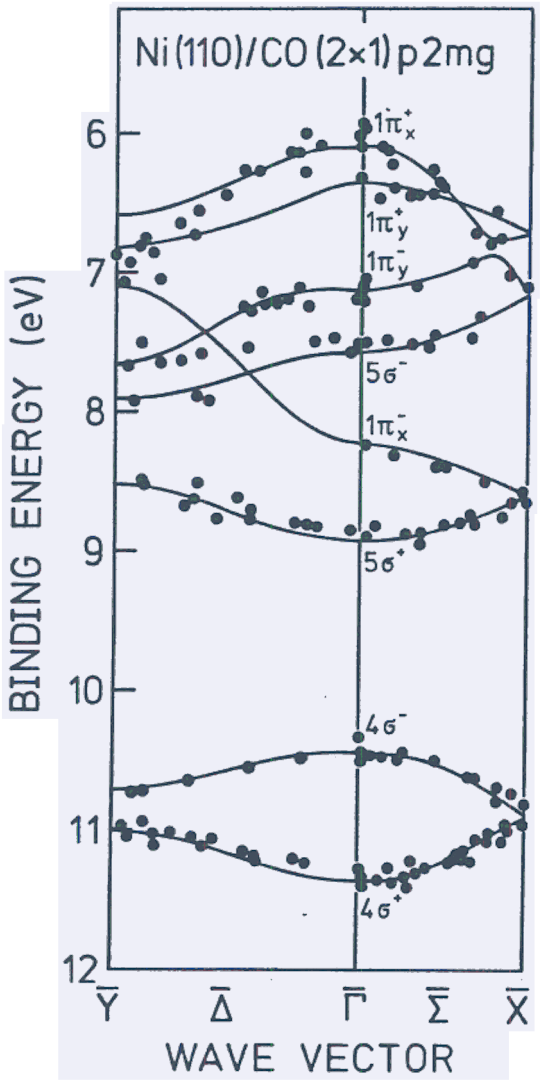


Fig. 23. Comparison of measured (circles) and calculated (full lines) quasi-two-dimensional band structure of the CO(2x1)p2mg/Ni(110) system (ref. 26).

before that not several such detailed theoretical analysis for various systems have been undertaken, an exponential decay for the 5σ band widths cannot be excluded. There is, yet, another interesting aspect of the p2mg band structure: The splitting between the two $1\pi_x$ derived bands at $\bar{\Gamma}$ is a strong function of the CO tilt angle with respect to the surface normal. Band structure calculations (ref. 26) as a function of the tilt angle showed that the optimum theoretical fit of the measured band structure can be obtained for a tilt angle of $17\pm2^{\circ}$. This value is in excellent agreement with results of other structure sensitive methods (refs. 150-151). It shows that similar to the gas phase, where photoelectron spectroscopy has been extensively used to determine, e.g. ring conformations (ref. 152),

adsorbate photoemission can be used in favourable cases to extract structural information.

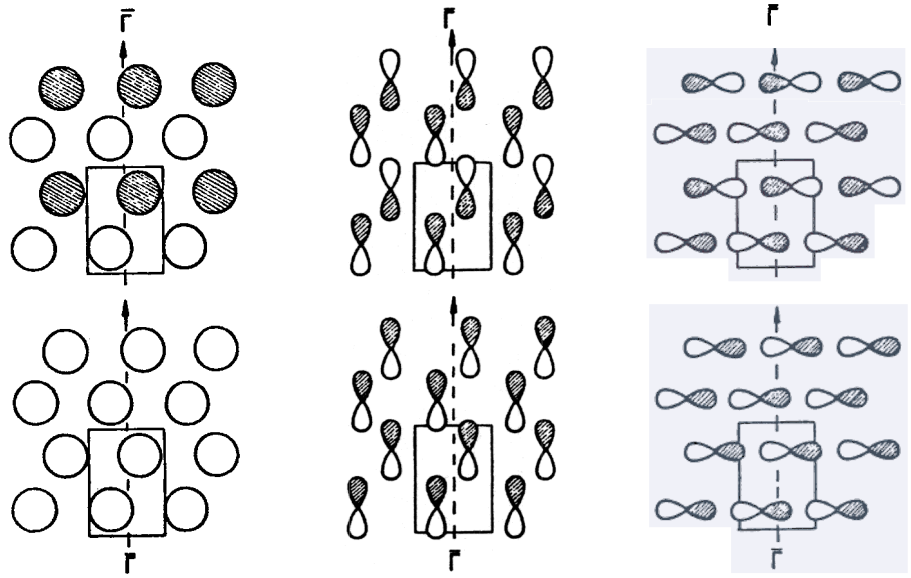

Fig. 24. Schematic representation of a CO-σ, and the two CO-π wavefunctions at $\bar{\Gamma}$ of a p2mg structure (ref. 26).

The examples for dispersions in quasi two dimensional systems were chosen so far from the many examples of strongly chemisorbed systems. One question is what happens to the dispersions when weakly chemisorbed or physisorbed systems are considered. The latter case is easy:
Fig.25 shows the dispersions measured via ARUPS for the system CO/Ag(111) (ref. 10). We know from the previous section that in this system the CO molecules are oriented with their axis parallel to the surface. It is known from LEED studies that CO molecules physisorbed on graphite form herring bone structures (ref. 153) as shown in the inset in Fig.25. Such structures again belong to nonsymmorphic space groups with two molecules in the unit cell. This is the reason why the molecular ionization bands appear as split in two components, i.e. a bonding and an antibonding combination at Γ. From symmetry considerations it is clear that these two bands are degenerate at the zone boundary. The splitting is larger for the σ levels than for the π level, which is not unreasonable on the basis of intermolecular overlap considerations. A particularly interesting observation has been made for this system if the temperature is increased. These physisorbed overlayers are known to undergo order-disorder transitions (ref. 153). The CO molecules are then no longer locked into a herring bone structure but rotate freely on their

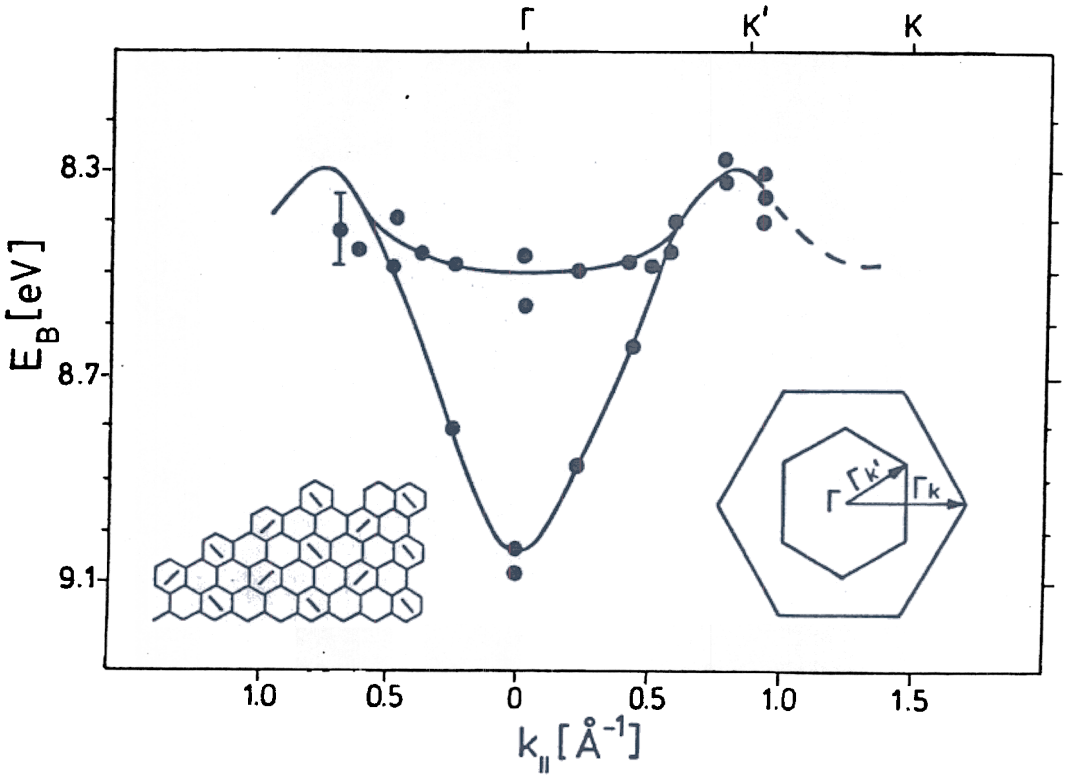


Fig. 25. $k_{\parallel}$ dispersion of the 5σ levels for the system CO/Ag(111) (ref. 10). The inset shows the assumed herring bone structure.

site. This destroys the nonsymmorphic structure and, concommitantly, the splitting of the σ levels disappears. CO/Ag(111) is a system where ARUPS can be used to study phase transitions in quasi-twodimensional systems (ref. 10).

In the case of weakly chemisorbed systems the situation is slightly more complicated:

The reason for this complication is the shake-up structure identified in the previous section (ref. 11). Fig.26 shows the dispersions for the system (√7x√7)CO/Cu(111), for which Fig.2 showed an electron distribution curve (ref. 11). In this case the CO molecules are oriented perpendicular to the surface as in the case of the strongly chemisorbed systems. While the integrated 5σ/1π dispersion is compatible with other CO overlayer systems, the 4σ dispersion is considerably smaller than expected for the given intermolecular separation. The observed value is represented in Fig.21 by the dashed circle. The shake-up which is- as noted above- associated with the 4σ ionization shows almost no dispersion, but a slight variation in relative intensity with respect to the 4σ ionization. There are sum-rules (ref. 154) relating intensity and ionization energy of

the peaks in the observed spectral function with the quasi-particle energy. These sum-rules are of the type:

$$\varepsilon_k^{HF} = \int_{-\infty}^{+\infty} \omega A(\omega,k)\,d\omega \qquad (5)$$

We can apply this sum rule to the observed data and regain a dispersion shown as the open circles in Fig.26. This renormalized 4σ band widths can now be favourably compared with the values measured for the strongly chemisorbed systems. This shows that it is the ionization process that introduces the deviations in the observed band widths and not a different intermolecular interaction potential in this case.

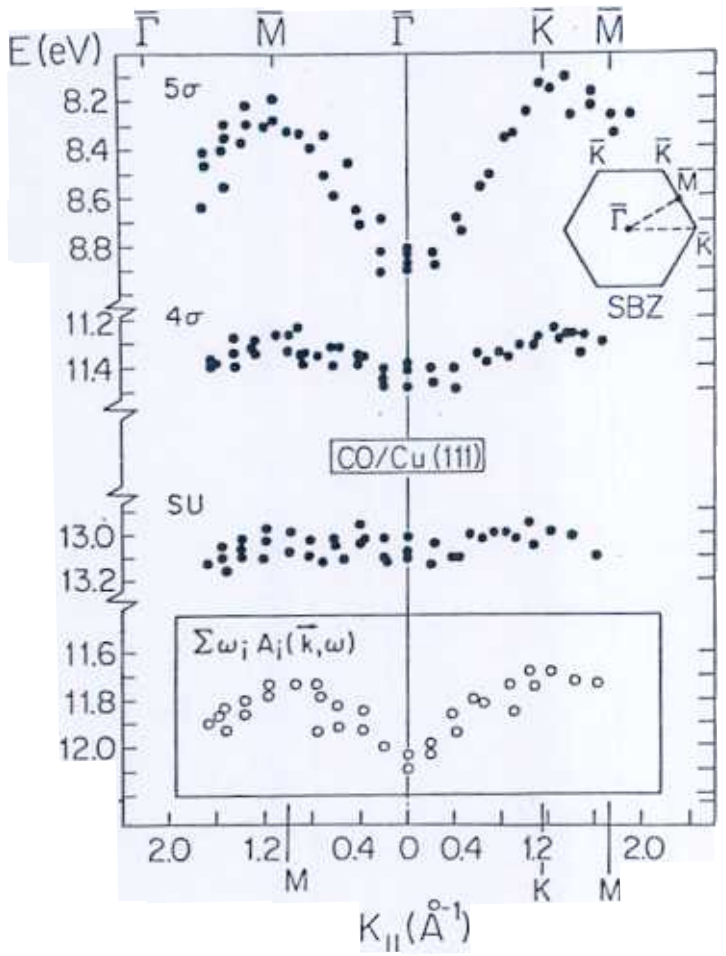


Fig. 26. $k_{\parallel}$ dispersions of the CO induced features (filled circles) for the system CO(√7x√7)/Cu(111) (ref. 11) including the 4σ satellite (see text). The dispersion calculated via the analysis of the spectral function according to equation (5) is shown as open circles (ref. 11).

A way to investigate the substrate mediated intermolecular interactions may be the analysis of the dispersion of the above mentioned molecule induced changes in the region of the metal substrate ionizations (see solid lines in the region of the

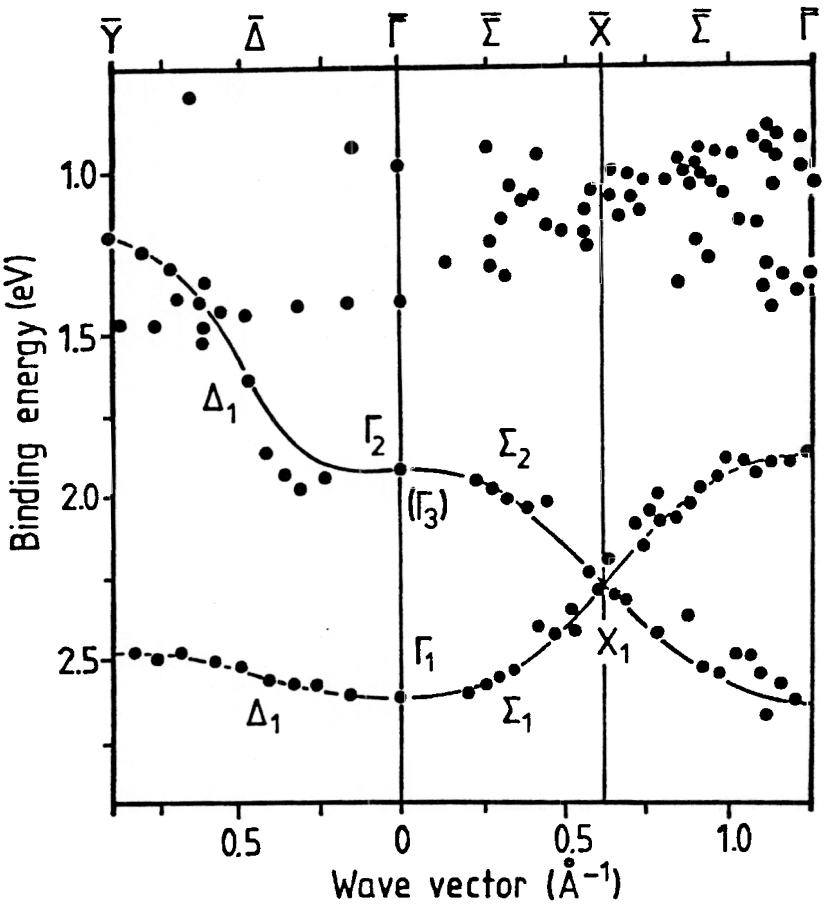


Fig. 27. $k_{\parallel}$ dispersions of the Ni3d-CO2π-back-bonding states in the region of the metal emissions in the system CO(2x1)p2mg/Ni(110) (ref.63). The full lines are the results of qualitative tight-binding estimations.

projected band structure in Fig. 1). Such an analysis has been carried out for the CO(2x1)p2mg/Ni(110) system (ref. 61). Before the dispersions are analysed we have to ensure that the bands are really localized at the surface of the solid,i.e. the CO2π-Ni3d features should not exhibit a dispersion as a function of photon energy in normal emission, which is the usually applied criterion for a surface state. Once this has been done, we can determine the dispersion via off normal emission and vary the photon energy such that we choose an appropriate cross section of the feature under consideration. The result of such a -very tedious- analysis has been carried out by Kuhlenbeck et al. (ref. 63) and is shown in Fig.27 for two directions of the Surface Brillouin Zone. There are two important qualitative features of the dispersion curves. First there are no band gaps at zone boundary $\bar{X}$, which -as Hund pointed out in 1936 (ref. 155)- is a consequence of the glide plane in the $\bar{\Sigma}$ direction. Secondly, the lower well resolved band can be fitted very well

with a tight binding type curve (full lines). A detailed discussion, for which we refer to the original literature (ref. 63), reveales a rather clear picture of the nature of the CO2π-Ni3d interaction. For the case Ni(110) this interaction creates new surface resonances positioned from 1 to 2.7 eV below the Fermi energy with the appropriate symmetry and intensity. This picture seems to be quite incompatible with the Newns-Anderson model (ref. 156) of CO chemisorption, where the CO2π orbital is resonantly broadened by interaction with the metal. The tails of this broadened band would extend below the Fermi energy and therefore create a degree of 2π occupancy. In contrast to the inadequacies of the Newns-Anderson model (ref. 156), it is quite easy to understand the data on the basis of the Blyholder model (ref. 4) used to explain Fig.1. In this model we have a 2π level, the width of which is not very important, far above the Fermi energy as the molecule approaches the surface. This level ( or the symmetry adapted combination of levels ) mixes into the metal levels because there is a finite overlap between them. Since the overlap is a matter of symmetry it determines which of the metal bands will couple with the CO2π. The question which of the 2π-induced bands are actually observed is then determined by the strength of the CO2π-metal coupling, and will depend upon the nature of the metal, the crystal face, and the structure of the CO layer.

Summarizing this section so far we have shown that ARUPS allows the observation of level specific dispersions. For those levels not strongly involved in the molecule-substrate interaction we can describe the measured dispersions by through space intermolecular interactions that depend exponentially on the intermolecular separation with a decay length of 1.25 Å independent of whether they are strongly or weakly chemisorbed. Chemisorbed systems cannot be compared with physisorbed systems because the adsorption geometry changes from perpendicular to parallel orientation. The observed dispersions reflect the global symmetry of the adsorbed layer, and can, in favourable cases, be used to obtain structural information of the adsorbed molecules. In certain systems the dispersion of metal-molecule-backbonding states can be observed.

Quasi-two-dimensional level dispersions have so far mainly been investigated for pure CO overlayers. Very recently, several

groups have started to study other systems. For example, the dispersions in $N_2$ overlayers on Ni(100) (ref. 73) and on Ni(110) (ref. 157) have been determined. Ordered NO adsorbates have recently been studied with ARUPS (refs. 158,159). Steinrück et al. (ref. 158) report on an interesting comparison of the size of the 4σ dispersions in the c(4x2)NO/Ni(111) and the c(4x2)CO/Ni(111) systems. They find relatively larger 4σ dispersions in the CO adsorbate.

3.2 Co-adsorbates

Some studies (refs. 34, 143, 147, 160-161) on co-adsorbate systems have been published very recently. In the following we briefly review what is known about band dispersions in ordered co-adsorbates.

The first molecular co-adsorbate system that has been studied with ARUPS with respect to level dispersions were ordered K/CO overlayers (refs. 34, 143, 161). The bandwidth found for the 4σ level is included in Fig.21 as the filled triangle. Unfortunately, the structure model for the co-adsorbate is not unique (ref. 160). The CO-CO distance used in the present case is based on the assumption that a (√3x√3)R30° CO overlayer is co-adsorbed with a (√3x√3)R30° K overlayer, which leads to the observed (3x3) overlayer structure (ref. 160). There are other structures possible, which would give shorter CO-CO distances, but the result would always lead to a relatively large band width as compared with pure CO overlayers. Obviously, the co-adsorption of K causes the 4σ wave function to change considerably, in the sense that the CO-CO interaction is mediated via the co-adsorbed potassium.

Very recently, an ordered CO/O co-adsorbate on Pd(111) has been studied using ARUPS (ref. 143). Early angle integrated photoemission results (ref. 162) were basically reproduced. The co-adsorption of oxygen shifts the positions of the 4σ and 5σ/1π bands to higher binding energies. This has been taken as evidence for a strong oxygen CO interaction. The ARUPS study shows that the 4σ dispersion, as presented in Fig.21 is in line with those of pure CO adsorbates. Therefore, if there is any distortion of the wavefunction it is smaller than in the case of K/CO adsorbates. Further comparison with other pure CO adsorbates on Pd(111) revealed that the observed chemical shift of the CO peaks can be explained exclusively via CO-CO

interaction. Therefore, the reason for the high tendency of the CO+O/Pd(111) system to form $CO_2$ well below room temperature (ref. 162) must be due to CO-CO and O-O repulsive interactions rather than strong attractive CO-O interactions within the adsorbate.

## 4. SYNOPSIS AND OUTLOOK

The present chapter shows that ARUPS is a very powerful tool to study the interaction of molecules on and with surfaces, with respect to geometric and electronic structure. Even relatively large molecules like aromatic hydrocarbons and their chemical reactions on surfaces have been successfully studied with this method in the past.

Often ordered molecular adsorbates can be used as model systems to study effects of more general physical importance. One promising area concerns the study of the influence of electronic correlations, i.e. many body effects, on energy-vs.-momentum disperions in periodic systems: In weakly chemisorbed, ordered molecular adsorbates particular ionizations exhibit intense satellite structure which leads to a breakdown of the band-like behaviour, while other ionizations in the same system may still show pronounced "normal" band dispersions (ref. 11). Our feeling is that more quantitative work should be done in this direction in the future.

Another interesting area of research in connection with molecular chemisorption is the study of many-electron-effects accompanying ionizations in the inner valence electron regime. Photoemission has not provided us so far with detailed spectroscopic information on this region where it is known from the gas phase that the simple one-electron picture of photoemission is known to break down. Although there have been some attempts (ref. 163) to study the inner valence electron regime, results have not been too promising. One reason for the problem may be that substrate emissions swamp the adsorbate features. Therefore experiments at the so called Cooper minimum (ref. 164) of the substrate cross sections could be appropriate to suppress such effects. Several groups have choosen a different approach (refs. 165-173): Angle resolved electron spectroscopy of ion states via autoionization of highly excited states of the adsorbate (sometimes unfortunately called

"Resonant Auger Decay"). Certainly, this will be one of the future directions to tackle this problem.

Also, we would like to mention a field which has been abandoned after some early work (ref. 174), namely the study of vibrational structure in photoemission of adsorbates. Especially for physisorbates at low temperature in connection with the study of phase transitions and desorption phenomena it should be possible to look for interesting aspects of the coupling between electronic and vibrational states. The investigation of molecular $H_2$ adsorbates could be of interest in this respect.

As mentioned in the introduction molecular chemisorption on semiconductor, metal oxides, and multi-component-system surfaces has not been studied with ARUPS to the same extent as metal surfaces. These, even technologically interesting systems should attract some attention in the near future.

Finally, with the advent of high brilliance and high flux light sources (ref. 175) it should be possible to excite photoelectrons in a highly localized spot on the adsorbate surface and still have sufficient intensity to do ARUPS of the emitted electrons. This may allow us to move towards the study of more realistic "adsorbate systems" and of adsorption at defects.

ACKNOWLEDGEMENTS

We would like to thank many colleagues and students for their help and support in carrying out some of the reviewed work. Among the many people we would like to mention in particular: B. Bartos, W. Eberhardt, G. Ertl, H.H. Graen, F. Greuter, M. Grunze, D. Heskett, G. Hohlneicher, G. Illing, H. Kuhlenbeck, R.P. Messmer, K. Müller, G. Odörfer, E.W. Plummer, H. Pulm, D. Saddei, W.R. Salaneck, D. Schmeisser, J. Wambach, G. Wedler. Mrs. H. Koslowski, Mrs. C. Risse, and Mr. H. Rayess are gratefully acknowledged for their technical support. H. Hamann has helped us by carefully reading the manuscript. Without the financial support of the Deutsche Forschungsgemeinschaft, the Bundesministerium für Forschung und Technologie, and the Fonds der Chemischen Industrie most of our own work could not have been carried out.

REFERENCES


1 D.E. Eastman, J.K. Cashion, Phys. Rev. Lett. 27, 1521 (1971).
2 E.W. Plummer, W. Eberhardt, Adv. Chem. Phys. 49,533(1982).
3 H.-J. Freund, M. Neumann, Appl. Phys. A47, 3 (1988).
4 N.V. Richardson, A.M. Bradshaw in: "Electron Spectroscopy"(Eds. C.R. Bundle und A.D. Baker), Vol. 4, (Acad. Press, N.Y. 1982).
5 G. Heiland, H. Lüth, Chapter 4 in "The Chemical Physics of Solid Surfaces and Heterogeneous Catalysis" (Eds. D.A. King, D.P. Woodruff) Vol.3, Elsevier (1982).
6 G. Blyholder, J. Phys. Chem. 68, 2772 (1968); G. Blyholder J. Vac. Sci. Technol. 11, 865 (1974).
7 C.M. Kao, R.P. Messmer, Phys. Rev. B31, 4835 (1985).
8 D.W. Turner, C. Baker, A.D. Baker, C.R. Brundle, "Molecular Photoelectron. Spectroscopy (Wiley, N.Y. 1970).
9 W. Eberhardt, H.-J. Freund, J. Chem. Phys. 78, 700 (1983).
10 D. Schmeisser, F. Greuter, E.W. Plummer, H.-J. Freund, Phys. Rev. Lett. 54, 2095 (1985).
11 H.-J. Freund, W. Eberhardt, D. Heskett, E.W. Plummer, Phys. Rev. Lett. 50, 768 (1983).
12 C.L. Allyn, Thesis, University of Pennsylvania (1978).
13 G. Odörfer, Diplomarbeit, Universität Erlangen-Nürnberg (1987).
14 CRC Handbook of Chemistry and Physics (Ed R.C. Weast), The Chemical Rubber Comp., 54th. Ed. (1973-1974).
15 G. McElhiney, H. Papp, J. Pritchard, Surf. Sc. 54, 617 (1976).
16 J. Kessler, F. Thieme, Surf. Sci. 67, 405 (1977).
17 K. Christmann, O. Schober, G. Ertl, J. Chem. Phys. 60, 4719. (1974)
18 H. Conrad, G. Ertl, J. Koch, E.E. Latta, Surf. Sci. 43, 462 (1974).
19 T.C. Chiang, G. Kaindl, D.E. Eastman, Sol. State Commun. 36, 25 (1980).
20 C.B. Duke, Surf. Sci. 70, 674 (1978).
21 C.B. Duke, W.R. Salaneck, F.-J. Fabisch, J.J. Ritsko, H.R. Thomas, A. Paton, Phys. Rev. B18, 5717 (1978).
22 J.W. Gadzuk, S. Holloway, K. Horn, C. Mariani, Phys. Rev. Lett. 48, 1288 (1982).
23 W.R. Salaneck, C.B. Duke, W. Eberhardt, E. W. Plummer, H.-J. Freund, Phys. Rev. Lett 45, 280 (1980).
24 C.L. Allyn, T. Gustafsson, E.W. Plummer, Chem. Phys. Lett. 47, 127 (1977).
25 K. Horn, A.M. Bradshaw, K. Jacobi, Surf. Sci. 72, 719 (1978).
26 H. Kuhlenbeck, M. Neumann, H.-J. Freund, Surf. Sci 173, 194 (1986).
27 F. Greuter, D. Heskett, E.W. Plummer, H.-J. Freund, Phys. Rev. B27, 7117 (1983).
28 E.S. Jensen, T. N. Rhodin, Phys. Rev. B27, 3338 (1983).
29 N.D. Shinn, J. Vac., Sci. Technol. A4, 1351 (1986).
30 R. Miranda, K. Wandelt, D. Rieger, R.D. Schnell, Surf. Sci.. 139, 430 (1984).
31 K. Horn, A.M. Bradshaw, K. Hermann, I.P. Batra, Sol. State Commun. 31, 257 (1979).
32 G. Borstel, M. Neumann, G. Seitz, W. Braun, Proc. 4th Intern. Conf. Sol. Surf., Vol. 1, p. 357 (Cannes, 1980).

33 P. Hofmann, J. Gossler, A. Zartner, M. Glanz, D. Menzel, Surf. Sci. 161, 303 (1985).
34 D. Heskett, E.W. Plummer, R.A. de Paola, W. Eberhardt, F.M. Hoffmann, Surf. Sci. 164, 490 (1985).
35 M. Steinkilberg, Thesis, Technical University München, (1977).
36 W. Braun, G. Meyer-Ehmsen, M. Neumann, E. Schwarz, Surf. Sci. 89, 354 (1979).
37 H. Kuhlenbeck, Diplomarbeit, Universität Osnabrück (1984).
38 C.W. Seabury, T.N. Rhodin, M. Traum, R. Benbow, Z. Hurych, Surf. Sci. 97, 363 (1980).
39 a) D. Rieger, R.D. Schnell, W. Steinmann, Surf. Sci. 143, 157 (1984).
b) P. Hofmann, S.R. Bare, D.A. King, Surf. Sci. 117, 245 (1982).
40 G. Apai, R.S. Wehner, R.W. Williams, J. Stöhr, D.A. Shirley, Phys. Rev. Lett. 37, 1497 (1976).
41 a) R.J. Smith. J. Anderson, G.J. Lapeyre, Phys. Rev. Lett. 37, 1081 (1976).
b) G.J. Lapeyre, J. Anderson, R.J. Smith, Surf. Sci. 89, 304 (1979).
42 I. Hermanson, Sol. State Commun. 22, 9 (1977).
43 a) K. Jacobi, M. Scheffler, K. Kambe, F. Forstmann, Sol. State Commun. 22, 17 (1977).
b) M. Scheffler, K. Kambe, F. Forstmann, Sol. State Commun. 25, 93 (1978).
44 L.S. Cederbaum, W. Domcke, Adv. Chem. Phys. 36, 205 (1977).
45 G. Borstel, M. Neumann, M. Wöhlecke, Phys. Rev. B23, 3121 (1981).
46 J.W. Davenport, Thesis, University of Pennsylvania, 1976; Phys. Rev. Lett. 36, 945 (1976).
47 E.W. Plummer, T. Gustafson, W. Gudat, D.E. Eastman, Phys. Rev. A15, 2339 (1977).
48 T. Gustafsson, Surf. Sci. 94, 593 (1980).
49 J. Wambach, Diplomarbeit, Universität Nürnberg-Erlangen (1987).
50 G. Paolucci, M. Surman, K.C. Prince, L. Sorba, A.M. Bradshaw, C.F. McConville, D.P. Woodruff, Phys. Rev. B34, 1340 (1986).
51 W. Wurth, C. Schneider, E. Umbach, D. Menzel, Phys. Rev. B34, 1336 (1986).
52 K. Hermann, P.S. Bagus, C.R. Brundle, D. Menzel, Phys. Rev. B24, 7025 (1981).
53 R.P. Messmer, S.H. Lamson, Chem. Phys. Lett. 65, 465 (1979).
54 H.-J. Freund, E.W. Plummer, Phys. Rev. B23, 4859 (1981).
55 K. Schönhammer, O. Gunnarsson, Sol. State Commun. 26, 399 (1978).
56 D. Saddei, H.-J. Freund, G. Hohlneicher, Surf. Sci. 95, 257 (1980).
57 G. Wendin "Structure and Bonding" Vol. 45 (Springer Verlag, Berlin (1981)).
58 D. Saddei, Thesis, Universität Köln (1982).
59 C. Mariani, H.-U. Middleman, M. Iwan, K. Horn, Chem. Phys. Lett. 93, 308 (1982).
60 H.P. Bonzel, private communication.
61 R.J. Smith, J. Anderson, G.J. Lapeyre, Phys. Rev. B22, 632 (1980).
62 T. Boszo, I. Arias, T.E. Yates, R.M. Martin. H. Metiu, Chem. Phys. Lett. 94, 243 (1983).

63 H. Kuhlenbeck, H.B. Saalfeld, M. Neumann, H.-J. Freund, E.W. Plummer, Appl. Phys. A44, 83 (1987).
64 W. Eberhardt, R. Cantor, F. Greuter, E.W. Plummer, Sol. State Comm. 42, 799 (1982).
65 a)K. Christmann, M. Ehsasi, K.H. Ernst, H. Kuhlenbeck, M. Neumann, H.B. Saalfeld, E. Schwarz, in "BESSY-Jahresbericht 1986", p.206.
b)K.H. Ernst, E. Schwarz, K. Christmann, H. Kuhlenbeck, M. Neumann, in "BESSY-Jahrebericht-1987", p.279.
66 B. Bartos, H.-J. Freund, H. Kuhlenbeck,. M. Neumann, unpublished, and ref. /70/.
67 C. Benndorf, B. Nieber, B. Krüger, Surf. Sci. 177, L907, (1986).
68 G. Ertl, J. Vac, Sci. Technol. A1, 1247 (1983).
69 M. Grunze, M. Golze, W. Hirschwald, H.-J. Freund. H. Pulm, U. Seip, N.C. Tsai, G. Ertl, F. Küppers, Phys. Rev. Lett. 53, 850 (1984).
70 H.-J. Freund, B. Bartos,. R.P. Messmer, M. Grunze, H. Kuhlenbeck, M. Neumann, Surf. Sci. 185, 187 (1987).
71 K. Horn, J.N. Di Nardo, W. Eberhardt, H.-J. Freund, E.W. Plummer, Surf. Sci. 118, 465 (1982).
72 E. Umbach, A. Schichl, D. Menzel, Sol. State Comm. 36, 93 (1980).
73 P.A. Dowben, Y. Sakisaka, T.N. Rhodin, Surf. Sci. 147, 89 (1984).
74 M.J. Breitschafter, E. Umbach, D. Menzel, Surf. Sci. 178, 725 (1986).
75 A. Schichl, D. Menzel, N. Rösch, Chem. Phys. 65, 225 (1982); Chem. Phys. Lett. 105, 285 (1984).
76 R.P. Messmer, J. Vac. Sci. Technol. A2, 899 (1984).
77 K.C. Prince, G. Paolucci, A. M. Bradshaw, Surf. Sci. 175, 101 (1986).
78 J.L. Grand, B.A. Sexton, G.B. Fisher, Surf. Sci. 95, 587 (1980).
79 H. Steininger, J. Lehwald, H. Ibach, Surf. Sci. 123, 1 (1982).
80 J.S. Somers, M.E. Kordesch, R. Hemmen, Th. Lindner, H. Conrad, A.M. Bradshaw, Surf. Sci. in press. (1988).
81 M.G. Ramsey, G. Rosina, F.P. Netzer, H.B. Saalfeld, D.R. Lloyd, Verhandl. DPG (VI) 23, 02.7 (1988).
82 F.P. Netzer, Surf. Sci. 52, 709 (1975).
83 K. Hermann, W. Müller, P.S. Bagus, J. Electr. Spectr. Rel. Phen. 39, 107 (1986).
84 J.A. Rodriguez, C.T. Campbell, Surf. Sci. 185, 299 (1987).
85 e.g. M.J. Breitschafter, E. Umbach, D. Menzel, Surf.Sci.109, 493, (1981).
J. Kanski, T.N. Rhodin, Surf. Sci. 65, 63 (1977).
H.P. Bonzel, G. Pirug, Surf. Sci 62, 45 (1977).
E. Umbach, S. Kulkarni, P. Feulner, D. Menzel, Surf. Sci. 88, 65 (1979).
86 G. Loubriel, Thesis, University of Pennsylvania, (1978).
87 H.-P. Steinrück, C. Schneider, P. Heimann, T. Posche, K. Eberle, E. Umbach, D. Menzel, Verhdl. DPG 23, 0-2.9 (1988).
88 a) E. Miyazaki, I. Kojima, M. Orita, K. Sawa, N. Sanada, K. Edamoto, T. Migakara, H. Kato, Surf. Sci. 176, L841 (1986).
b) E. Miyazaki, I. Kojima, M. Orita, K. Sawa, N. Sanada, K. Edamoto, T. Migakara, H. Kato, J. Electr. Spectr. Rel. Phen. 43, 139 (1987).
89 F.A. Cotton, G. Wilkinson, "Advanced Inorganic, Chemistry", Fourth Edition, John Wiley & Sons, N.Y. (1980).
90 e.g. P.R. Norton, P.J. Richards, Surf. Sci. 49, 567 (1975)

91 e.g. J. Fuggle, D. Menzel, M. Kiskinova, G. Pirug, H.P (1984).
92 e.g. C.R. Brundle, J. Vac.
93 B. Bartos, H.-J. Freund, H. Lindner, K. Müller, Surf. S
94 H.-J. Freund, H. Behner, B. Kuhlenbeck, M. Neumann, Sur
95 B. Bartos, H.-J. Freund, H. Springer Series in Surface Interface Reactions" (Eds. ,Springer Verlag Berlin (19
96 H.-J. Freund, R.P. Messmer,
97 K.C. Prince, A.M. Bradshaw,
98 K.C. Prince, G. Paolucci, J 181 (1985).
99 P. Hofmann, D. Menzel, Surf
100 Th. Lindner, J. Somers, A.M Sci. 185, 75 (1987).
101 S.D. Peyerimhoff, J. Chem.
102 P.A. Thiel, T.E. Madey, Sur
103 C. Nöbl, C. Benndorf, T.E. (1985).
104 C. Benndorf, T.E. Madey, Su
105 R.J. Purtell, R.P. Merrill, Phys. Rev. Lett. 44, 1278 (
106 K. Jacobi, E.S. Jensen, T.N. (1981).
107 C.W. Seabury, T.N. Rhodin, Surf. Sci. 93, 117 (1980).
108 M.W. Kang, C.H. Li, S.Y. Tor R.J. Purtell, R.P. Merrill, (1981).
109 M.R. Albert, L.G. Sneddon, T.Gustafsson, E.W. Plummer,
110 K. Horn, A.M. Bradshaw, K. J 15, 575 (1978).
111 P. Hoffmann, K. Horn, A. Gar in ref. 3.
112 P. Hoffmann, K. Horn, A.M. E (1981).
113 F.P. Netzer, J.U. Mack, J. C
114 M. Neumann, J.U. Mack, E. Be Sci.155, 629 (1985).
115 F.P. Netzer, G. Rosina, E. B Sci. 184, L 397 (1987).
116 F.P. Netzer, H.H. Graen, H. Phys. Lett. 133, 49 (1987).
117 F.P. Netzer, G. Rangelov, G. Neumann, D.R. Lloyd, Phys. R
118 J.U. Mack, E. Bertel, F.P. N (1985).
119 H.H. Graen, M. Neuber, M. Ne F.P. Netzer, J. Chem. Phys.
120 J. Somers, M.E. Bridge, D.R. 181, L 167 (1987).
121 W. Sesselmann, B. Woratschek Haberland, Surf. Sci. 130, 2
122 W.T. Tysoe, G.L. Nyberg, R.M (1983).

123 P. Yannoulis, E.E. Koch, M. Lähdeminhi, Surf. Sci. 182, 299 (1987).
124 R. Klauser, M. Surman, Th. Lindner, A.M. Bradshaw, Surf. Sci. 183, L279 (1987).
125 D.W. Goodman, J.T. Yates, T.E. Madey, Surf. Sci. 93, L 135 (1980).
126 C.L. Allyn, T. Gustafsson, E.W. Plummer, Sol. State Comm. 24, 531 (1977).
127 H.P. Bonzel, Surf. Sci. Rep. 8, 43 (1988).
128 W. Eberhardt, F.M. Hoffmann, R. DePaola, D. Heskett, I. Strathy, E.W. Plummer, H.R. Moser, Phys. Rev. Lett. 54, 1856 (1985).
129 D. Heskett, E.W. Plummer, Phys. Rev. B33, 2322 (1986).
130 D. Heskett, I. Strathy, E.W. Plummer, R.A. Depaola, Phys. Rev. B32, 6222 (1985).
131 D. Heskett, E.W. Plummer, R.A. Depaola, W. Eberhardt, Phys. Rev. B33, 5171 (1986).
132 J.J. Weimer, E. Umbach, Phys. Rev. B30, 4863 (1984).
133 J.J. Weimer, E. Umbach, D. Menzel, Surf. Sci. 159, 83 (1985).
134 W. Wurth, J.J. Weimer, E. Hudeczek, E. Umbach, Surf. Sci. 173, L 619 (1986).
135 M. Kiskinova, G. Pirug, H.P. Bonzel, Surf. Sci. 133, 321 (1983).
136 G. Broden, G. Gaffner, H.P. Bonzel, Surf. Sci. 84, 295 (1979).
137 R.A. DePaola, F.M. Hoffmann, D. Heskett, E.W. Plummer, to be published.
138 J. Wambach, G. Odörfer, H.-J. Freund, H. Kuhlenbeck, M. Neumann, Surf. Sci. to be published.
139 G. Rosina, G. Rangelov, E. Bertel, H. Saalfeld, F.P. Netzer, Chem. Phys. Lett. 140, 200 (1987).
140 R. Hemmen, M.E. Kordesch, H. Conrad, Surf. Sci. , to be published.
141 H. Pulm, B. Marquardt, H.-J. Freund,R. Engelhardt, K. Seki, U. Karlsson, E.E. Koch, W. v. Niessen, Chem. Phys. 92, 457 (1985).
142 E.W. Plummer, private communication.
143 G. Odörfer, E.W. Plummer, H.-J. Freund, H. Kuhlenbeck, M. Neumann, Surf. Sci. 198, 331 (1988).
144 K. Horn, M. Scheffler, A.M. Bradshaw, Phys. Rev. Lett. 41, 822 (1978).
145 I.P. Batra, K. Hermann, A.M. Bradshaw, K. Horn, Phys. Rev. B20, 801 (1979).
146 C.W. Seaburg, E.S. Jensen, T.N. Rhodin, Sol. State Comm. 37, 383 (1981).
147 D. Heskett, private communication.
148 C. Schneider, H.-P. Steinrück, P. Heimann, T. Pache, M. Glanz, K. Eberle, E. Umbach, D. Menzel, Verhdl. DPG O-24.4 (1988).
149 A review collecting experimental information gained via photoemission on systems belonging to non-symmorphic space groups has recently been published by K.C. Prince, J. Electr. Spectr. Rel. Phen. 42, 217 (1987), and we refer to this paper for details.
150 W. Riedl, D. Menzel, Surf. Sci. 163, 39 (1985).
151 Very recent X-ray-photoelectron diffraction results by D. Wesner, F.P. Koenen, H.-P. Bonzel Phys. Rev. Lett. 60, 1045 (1988), and U. Buskotte, M. Neumann to be published confirm this angle.

152 R.S. Brown, F.S. Jorgensen in "Electron spectroscopy" Vol 5 (Ed. D.A. Baker, C.R. Brundle), Acad. Press, London 1984) p.2.
153 R.D. Diehl, S.C. Fain, Surf. Sci. 125, 116 (1983).
154 L. Hedin, Phys. Sci. 21, 477 (1979); B.I. Lundquist, Phys. Kond. Mater. 6, 193, 203 (1967), and 7, 117 (1968), and 9, 2236 (1969).
155 F. Hund, Z. Phys. 99, 119 (1936).
156 D.M. Newns, Phys. Rev. 178, 1123 (1969).
157 H. Kuhlenbeck, M. Neumann, H.-J. Freund, unpublished.
158 H.-P. Steinrück, C. Schneider, P. Heimann, T. Pache, E. Umbach, D. Menzel, Surf. Sci., to be published.
159 G. Odörfer, R. Jaeger, H. Geissler, H. Kuhlenbeck, H.-J. Freund, M. Neumann, unpublished results.
160 J.J. Weimer, E. Umbach, D. Menzel, Surf. Sci. 159, 83 (1985).
161 H.P. Steinrück, E. Umbach, D. Menzel, private communication.
162 H. Conrad, G. Ertl, J. Küppers, Surf. Sci. 76, 323 (1978).
163 H.-J. Freund, F. Greuter, D. Heskett, E.W. Plummer, Phys. Rev. B28, 1727 (1983).
164 J.W.Cooper, Phys. Rev. 128, 681 (1962).
165 C.T. Chen, Thesis, University of Pennsylvania (1985), unpublished.
166 E.W. Plummer, C.T. Chen, W.K. Ford, W. Eberhardt, R.P. Messmer, H.-J. Freund, Surf. Sci., 158, 58 (1985).
167 C.T. Chen, R.A. DiDio, W.K. Ford, E.W. Plummer, Phys. Rev. B32, 8434 (1985).
168 D. Menzel, P. Feulner, R. Treichler, E. Umbach, W. Wurth, Phys. Scr. T17, 166 (1987).
169 W. Eberhardt, Phys. Scr. T17, 28 (1987).
170 G. Loubriel, T. Gustafsson, L.I. Johansson, S.J. Oh, Phys. Rev. Lett. 49, 571 (1982).
171 W. Wurth, R. Treichler, E. Umbach, D. Menzel, Phys. Rev. B35, 7741 (1987).
172 W. Wurth, C. Schneider, R. Treichler, D. Menzel, E. Umbach, Phys. Rev. B37, 8725 (1988).
173 G. Illing, T. Porwol, H.-J. Freund, H. Kuhlenbeck, M. Neumann, S. Bernstorff, Proc. 3rd Surf. Sci. Symp., Kaprun, Austria, p.81 (1988).
174 W. Eberhardt, E.W. Plummer, Phys. Rev. Lett. 47, 1476 (1981).
175 Technical Report:"BESSY II- Eine optimierte Undulator/Wiggler Speicherring Lichtquelle für den VUV und XUV-Spektralbereich.(Eds. A.Gaupp, E.E. Koch, R. Maier) (1986).